JAHRBUCH DER GEOLOGISCHEN BUNDESANSTALT

Jb. Geol. B.-A. | ISSN 0016-7800 | Band 147 | Heft 3+4 | S. 527–544 | Wien, Dezember 2007

Two-mica Granites of the Plechý (Plöckenstein) Pluton in the Triple-Point Area (Trojmezí, Dreiländereck) of Austria, the Czech Republic, and Germany

KAREL BREITER*), FRIEDRICH KOLLER**), SUSANNA SCHARBERT***), WOLFGANG SIEBEL****), RADEK ŠKODA*****) & WOLFGANG FRANK******)

15 Text-Figures, 10 Tables

Deutschland
Tscheichische Republik
Oberösterreich
Moldanubikum
Plöckenstein-Pluton
Radioaktivität
Geochemie
Geochronologie

Österreichische Karte 1 : 50.000
Blätter 2, 3, 13, 14

Content

Die Zweiglimmer-Granite des Plöckenstein-Plutons am Dreiländereck Österreich – Tschechische Republik – Deutschland

Zusammenfassung

Der Plöckenstein-Pluton bildet einen elliptischen Stock, etwa 13 x 10 km groß, im Dreiländereckgebiet Oberösterreich – Tschechische Republik – Bayern. Der Pluton ist geologisch jünger als alle umliegenden magmatischen Gesteine (porphyrischer Amphybol-Biotit-Syenit, biotitreicher Weinsberger Granit und feinkörnige Biotit- und Zweiglimmergranite). Geologische Kartierungen ergaben drei verschiedene Granittypen:

*) KAREL BREITER, Czech Geological Survey, Geologická 6, CZ 15200 Praha 5; Geological Institute of the Academy of Science of the Czech Republic v.v.i., Rozvojová 257, CZ 16500 Praha 6.
breiter@gli.cas.cz.
**) FRIEDRICH KOLLER, Department of Lithospheric Research, University of Vienna, Althanstraße 4, A 1090 Wien.
***) SUSANNA SCHARBERT, Geologische Bundesanstalt, Neulinggasse 38, A 1030 Wien.
****) WOLFGANG SIEBEL, Tübingen University, Wilhelmstrasse 56, D 72074 Tübingen.
*****) RADEK ŠKODA, Masaryk University, Kotlářská 2, CZ 60000 Brno.
******) WOLFGANG FRANK, CEAL Laboratory, Geologický ústav SAV, Dúbravská cesta 9, SK 84005 Bratislava.

1) Plöckenstein-Granit: Ein grobkörniger Zweiglimmergranit bildet den größten Teil des Plutons.
2) Dreisesselgranit: Ein porphyritisch-grobkörniger Zweiglimmergranit bildet einen N–S-verlaufenden Körper im westlichen Teil des Plutons mit den Gipfeln Hochstein and Dreisessel.
3) Steinberggranit: Ein hiatalporphyritischer Zweiglimmergranit mit fein- bis mittelkörnigen Grundmasse bildet einen halbmondförmigen Körper im südlichen und südwestlichen Teil des Plutons. Eine markante Orientierung der Orthoklaseinsprenglinge ist für diesen Granit typisch..

Alle drei Granit-Typen sind peralumin (ASI: 1,15–1,25). Plöckenstein- and Dreisessel-Granite sind chemisch relativ homogen, mit 72–74 Gew.-% SiO_2, 1,2–1.7 Gew.-% Fe_2O_3tot, 0,1–0,3 Gew.-% MgO, 0,5–0,6 Gew.-% CaO, 4,8-5,2 Gew.-% K_2O, und 3–4 % Gew.-% Na_2O. Die Spurenelemente schwanken zwischen 300–400 ppm Rb, 40–80 ppm Zr und 10–20 ppm Th. Der Steinberggranit enthält weniger Silizium (70,5–72,0 Gew.-% SiO_2) und Natrium (2,6–3,1-Gew.-%) und mehr Fe_2O_3tot (1,8–2,5 Gew.-%), MgO (0,3–0,6 Gew.-%), CaO (0,7–1,0 Gew.-%), and K_2O (4,8–6,2 Gew.-%) im Vergleich mit Plöckenstein- und Dreisessel-Granit. Bemerkenswert ist eine Anreicherung von Zr (130–220 ppm) und besonders von Th (40–90 ppm).

Die mineralogische Zusammensetzung aller drei Granite ist ähnlich: Quarz, perthitischer K-Feldspat, Albit-Oligoklas, Biotit und primärer Muskovit. Apatit, Zirkon, Monazit und Ti-Oxide sind häufige Akzessorien. Die Anreicherung von Thorium im Steinberggranit ist mit einem häufigen Vorkommen des Minerals Monazit (bis 28 Gew.-% ThO_2) verknüpft.

Einzelne Zirkon-Verdampfungs-Alter (laufendes Projekt, SIEBEL et al., in Vorb.) aller drei Granite liegen in einem engen Intervall von 328–325 Ma. Die Ar-Ar- und Rb-Sr-Alter der Glimmer legen die Abkühlung des Plutons zwischen 327 und 309 Ma. fest.

Der porphyrische Dreisesselgranit wird als Dachfazies des Plöckenstenplutons interpretiert, die nach unten allmählich in den typischen grobkörnigen Plöckensteingranit übergeht. Der Steinberggranit ist eine unabhängige, etwas ältere, wenig fraktionierte Intrusion.

Abstract

The Plechý/Plöckenstein pluton forms an elliptical stock, 13 x 10 km in size, around the triple-point of Austria, the Czech Republic, and Germany. It is geologically younger than the neighbouring granitoids including the melasyenites, the Weinsberg granite, and the fine-grained biotite- to two-mica granite. Three main granite types can be distinguished within the pluton.

1) Plechý/Plöckenstein granite: a generally equigranular, coarse-grained two-mica granite which forms the major part of the pluton.
2) Dreisessel granite: a serialporphyritic, coarse-grained two-mica granite which forms a N–S-elongated body in the western part of the pluton and the summit of the Hochstein and Dreisessel/Třístoličník.
3) Steinberg granite: a hiatalporphyritic two-mica granite with a medium-grained groundmass which forms a crescent-like body in the southern and south-western part of the pluton. The strong alignment of K-feldspar phenocrysts is characteristic for this granite.

All granite types are peraluminous (ASI: 1.15–1.25). The granites of the Plechý and Dreisessel types are chemically relatively homogeneous, with 72–74 wt.% SiO_2, 1.2–1.7 wt.% Fe_2O_3tot, 0.1–0.3 wt.% MgO, 0.5–0.6 wt.% CaO, 4.8–5.2 wt.% K_2O, and 3–4 wt.% Na_2O. Trace elements range between 300–400 ppm Rb, 40–80 ppm Zr, and 10–20 ppm Th. The Steinberg granite has less silica (SiO_2 70.5–72.0 wt.%) and Na_2O (2.6–3.1 wt.%), and higher Fe_2O_3tot (1.8–2.5 wt.%), MgO (0.3–0.6 wt.%), CaO (0.7–1.0 wt.%), and K_2O (4.8–6.2 wt.%) compared to the Plechý and Dreisessel granite types. Its enrichment in Zr (130–220 ppm) and, especially, in Th (40–90 ppm) is remarkable.

The mineralogical composition of all three granite types is similar: quartz, perthitic K-feldspar, albite-oligoclase, biotite, and primary muscovite. Among the accessory and opaque minerals, apatite, zircon, monazite, and Ti-oxides are common. Enrichment of thorium in the Steinberg granite is mineralogically expressed by a high modal abundance of monazite (up to 28 wt.% ThO_2).

In a companion study (SIEBEL et al., in prep.) single-zircon Pb-Pb evaporation ages ranging from 328 to 325 Ma were determined for the three granites. Ages obtained by the Ar-Ar and Rb-Sr methods on micas indicate cooling of the pluton between 327 and 309 Ma.

The Dreisessel granite is interpreted as the near-upper contact facies of the Plechý pluton, slowly passing down into the typical equigranular Plechý granite. The Steinberg granite forms a separate, slightly older, less-differentiated intrusion.

1. Introduction

The Triple-Point Area (Dreiländereck, Trojmezí) is a mountainous and forest-covered landscape in the border area of Austria, the Czech Republic, and Germany, situated approximately between the Vltava (Moldau) valley to the NE and the Mühl fault zone to the SW. Geological maps at different scales exist on the territories of all three states: 1 : 75 000 in Austria (THIELE & FUCHS, 1965), 1 : 50 000 in the Czech Republic (MIKSA & OPLETAL 1995), and 1 : 25 000 in Germany (OTT, 1992), but mutual comparison of these three maps is still problematical. A first attempt to connect Austrian and Czech geological knowledge and maps has been done in the framework of cooperation between the Geologische Bundesanstalt, Wien, and the Czech Geological Survey, Praha (Breiter and Scharbert, unpublished; Geological Map of Oberösterreich)

New geological mapping of the territory of the Šumava National Park (Bohemian Forest) on a scale of 1 : 25 000, conducted by the Czech Geological Survey (PERTOLDOVÁ et al., 2004; BREITER & PERTOLDOVÁ, 2004; PERTOLDOVÁ, 2006) improved the knowledge about the distribution of individual rock types in the Czech part of the area. Detailed measurement of radioactivity on the Austrian and Czech territory could identify a thorium-rich variety of the two-mica, Eisgarn-type granite near Oberschwarzenberg (BREITER, 2005). Recently, petrological investigation and small-scale mapping, supported by the Austrian-Czech project KONTAKT in 2005–2006, allowed to interconnect the geological maps in all three states (BREITER & KOLLER, 2005).

The Triple-Point Area is part of the Moldanubian zone of the Bohemian Massif. It is formed by amphibolite-facies metamorphic rock intruded by several types of Variscan granitoids, including K- and Mg-rich melasyenites (durbachites), porphyritic biotite granites (Weinsberg-type), fine-grained, locally deformed biotite to two-mica granites, and coarse-grained, locally porphyritic two-mica granites of the Plechý/Plöckenstein pluton.

The aim of this article is to decipher the internal structure of the Plechý/Plöckenstein pluton, to describe individual granite types within the pluton, their mineral and chemical composition, and to establish individual intrusions and their age relationships.

2. Geology of the Plechý/Plöckenstein Pluton

The Plechý/Plöckenstein pluton forms an elliptical stock, 13×10 km in size, elongated in SW–NE direction around the triple-point of Austria, the Czech Republic and Germany (Fig. 1). The southwest border of the pluton is tec-

Text-Fig. 1.
Simplified geological map and distribution of Th in the Plechý/Plöckenstein pluton.

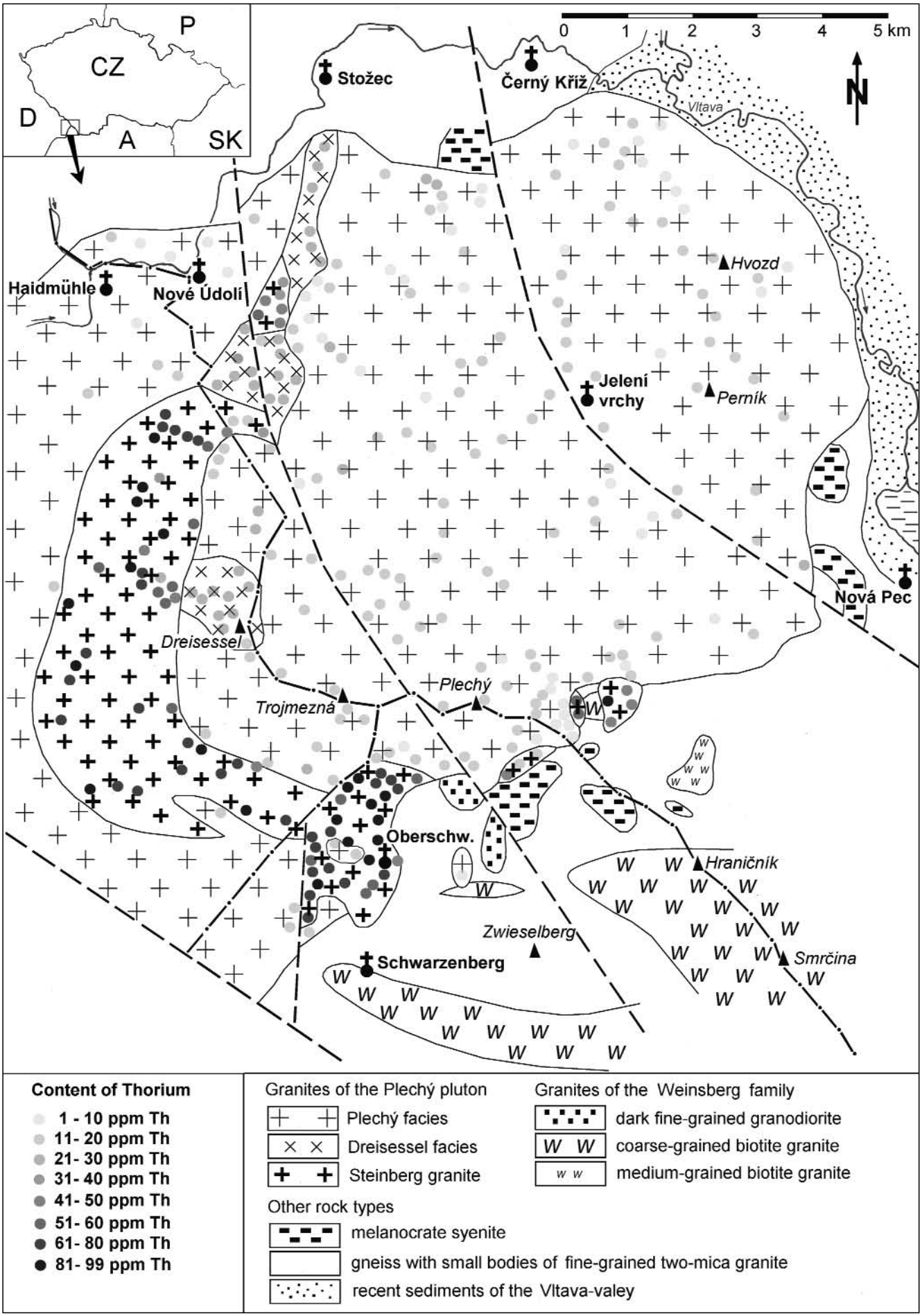
P
CZ
D
A
SK
0 1 2 3 4 5 km
N
Stožec
Černý Kříž
Vltava
Haidmühle
Nové Údolí
Hvozd
Jelení vrchy
Perník
Nová Pec
Dreisessel
Plechý
Trojmezná
Oberschw.
Hraničník
Zwieselberg
Schwarzenberg
Smrčina
Content of Thorium
1 - 10 ppm Th
11- 20 ppm Th
21- 30 ppm Th
31- 40 ppm Th
41- 50 ppm Th
51- 60 ppm Th
61- 80 ppm Th
81- 99 ppm Th
Granites of the Plechý pluton
Plechý facies
Dreisessel facies
Steinberg granite
Granites of the Weinsberg family
dark fine-grained granodiorite
coarse-grained biotite granite
medium-grained biotite granite
Other rock types
melanocrate syenite
gneiss with small bodies of fine-grained two-mica granite
recent sediments of the Vltava-valey

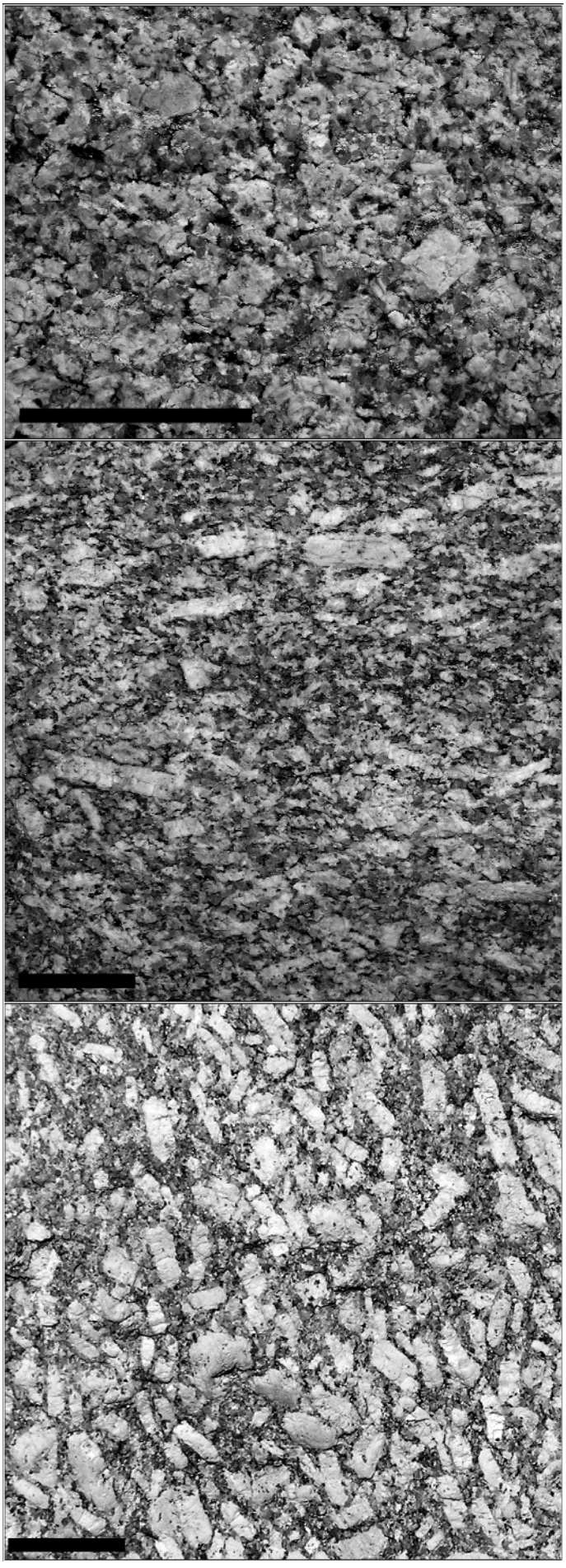

Text-Fig. 2.
Textures from various granite types of the Plechý/Plöckenstein pluton. From top to bottom: a = Plechý type; b = Dreisessel type; c = Steinberg type.
All scale bars 5 cm

tonic (Bavarian Pfahl), the NE contact is covered by Quaternary sediments of Vltava/Moldau valley, the eastern, south-eastern and western contacts are intrusive. The Plechý pluton is geologically younger than all neighbouring granitoids including the melasyenites, the Weinsberg granite, and the fine-grained biotite to two-mica granite. According to gravity measurements (BLÍŽKOVSKÝ & NOVOTNÝ 1982), the Plechý pluton forms one of the most intensive negative gravity anomalies in the Moldanubian zone, which appears to demonstrate very deep roots for this granite. Based on its geological and petrographic similarities with the Eisgarn granite s.s. from the area north of Gmünd (K-feldspar phenocrysts, plagioclase An_{2-10}, presence of biotite and muscovite), the Plechý granite was traditionally classified as Eisgarn-type granite (THIELE & FUCHS, 1965).

While the Austrian part of the pluton was described as a monotonous, coarse-grained two-mica granite (THIELE & FUCHS, 1965), two facies were distinguished in the Czech and German parts: an equigranular, coarse-grained, and a porphyritic variety (OTT, 1992; MIKSA & OPLETAL, 1995).

According to our investigation, three main granite facies (or types) can be distinguished within the pluton:

1) A generally equigranular, coarse-grained, locally weakly porphyritic two-mica granite (Text-Fig. 2a) forms the major part of the pluton. This granite should be, in agreement with older maps, termed as Plechý/Plöckenstein granite.
2) A serialporphyritic, coarse-grained two-mica granite (Text-Fig. 2b) forms a N–S elongated body in the western part of the pluton. It also forms the summit of the Hochstein and Dreisessel/Třístoličník. Porphyritic granites on summits of several hills in the western part of the pluton probably also belong to this type. K-feldspar phenocrysts are not aligned. We propose the name Dreisessel granite for this granite (see also chapter Discussion).
3) A hiatalporphyritic two-mica granite with a medium-grained groundmass (Text-Fig. 2c) forms a crescent-like body in the southern and southwestern part of the pluton. The characteristic feature of this granite is the strong alignment of K-feldspar phenocrysts. Another important feature is the high thorium concentration ranging between 40 and 90 ppm. This granite was firstly described from its western part in Bavaria as „Steinberg granite“ (OTT, 1992), thought without knowledge about its high Th-content. We adopt this local name for the whole intrusion (see chapter Discussion).

The mineralogical composition of all three granite types is similar: quartz, perthitic K-feldspar, plagioclase of albite-oligoclase composition, biotite and muscovite. Among the accessory and opaque minerals, apatite, zircon, monazite, and Ti-oxides are common.

Contact relations between the three different granite types have not been observed in the field. Dyke rocks turned out to be rare. Small blocks of fine-grained two-mica to aplitic muscovite granite were found in the southern part of the Plechý granite, in a broader area around Plešné Jezero lake. The striking direction of those dykes could not been determined.

Table 1.
Whole-rock chemical composition of studied granites. Major elements in wt.% (classical wet chemistry in laboratory of CGS Praha), trace elements in ppm (ICP-MS in laboratory ACME Vancouver).
Localisation of samples: 3612 = Plechý granite, boulder 300 m to the south of the railway stop Pěkná, Czech Republic; 3623 = Plechý granite, small quarry at the Schwarzenberg water canal, Rossbach, Czech Republic; 4368 = Plechý granite, boulder 50 m to the south from the summit of Trojmezná (Bayerischer Plöckenstein), Germany; 4454 = aplitic dyke granite, outcrop 300 m to the west from the Plešné Jezero lake, Czech Republic; 4370 = slightly porphyritic Plechý granite, outcrop at the „Minister" way, Czech Republic; 4363 = Dreisessel granite, outcrop on the summit of Dreisessel mountain, Germany; 4364 = Dreisessel granite, outcrop on the summit of Hochstein, Germany; 4365 = Dreisessel granite, outcrop on the summit of Kamenná, Czech Republic; 3698 = Steinberg granite, road-cut at the ski bridge, Habergrasberg, Germany; 4139 = Steinberg granite, quarry Teufelschüssel, Austria; 4362 = Steinberg granite, boulder on the summit of Habergrasberg, Germany; 4369 = Steinberg granite, boulder on the summit of Špičák, Czech Republic.

Rock type	Plechý granite			Plechý-aplitic dyke	transition Plechý-Dreisessel	Dreisessel granite			Steinberg granite			
No.	3612	3623	4368	4454	4370	4363	4364	4365	3698	4139	4362	4369
SiO_2	73.18	73.53	73.60	74.02	73.67	73.22	74.25	72.41	70.27	71.46	71.83	72.86
TiO_2	0.16	0.25	0.16	0.04	0.21	0.22	0.18	0.22	0.37	0.49	0.32	0.37
Al_2O_3	14.94	13.73	14.35	14.76	13.89	13.98	13.73	14.31	14.80	14.22	14.53	13.63
Fe_2O_3	0.41	0.60	0.53	0.11	0.54	0.70	0.65	0.58	0.51	0.78	0.64	0.59
FeO	0.76	1.09	0.65	0.26	1.06	0.85	0.77	1.01	1.36	1.45	1.21	1.45
MgO	0.25	0.30	0.24	0.05	0.25	0.29	0.23	0.27	0.04	0.56	0.35	0.43
MnO	0.034	0.036	0.026	0.014	0.045	0.028	0.028	0.036	0.430	0.035	0.034	0.038
CaO	0.58	0.62	0.57	0.24	0.63	0.62	0.53	0.79	0.69	0.85	0.72	0.67
Li_2O	0.044	0.036	0.02	0.007	0.033	0.032	0.025	0.037	0.033	0.022	0.027	0.026
Na_2O	3.56	3.00	3.11	2.47	3.13	2.56	2.91	3.40	3.17	2.77	2.92	2.66
K_2O	4.85	4.88	5.32	6.70	4.64	5.26	4.88	4.99	5.47	5.53	5.21	5.41
P_2O_5	0.324	0.283	0.294	0.317	0.383	0.359	0.306	0.388	0.366	0.332	0.439	0.358
F	0.131	0.177	0.164	0.051	0.218	0.334	0.303	0.351	0.360	0.368	0.316	0.248
LOI	1.04	0.98	0.88	0.62	0.96	1.29	1.00	1.09	1.17	1.02	1.29	0.98
H_2O-	0.12	0.15	0.1	0.07	0.16	0.22	0.12	0.15	0.11	0.16	0.18	0.14
-F eq.	0.155	0.075	0.069	0.021	0.092	0.141	0.128	0.148	0.152	0.155	0.133	0.104
TOTAL	100.32	99.59	100.01	99.73	99.82	99.98	99.91	100.03	99.00	100.05	100.00	99.87
ASI	1.23	1.21	1.20	1.26	1.23	1.27	1.24	1.15	1.19	1.18	1.24	1.19
Ba	153	108	163	23	85	105	78	100	234	287	121	179
Be	8	7	4	5	3	5	5	8	8	9	7	6
Cs	35	29	16	6	21	13	13	26	28	13	14	11
Ga	24	24	23	24	28	28	26	26	28	28	26	28
Hf	1.9	3.6	2.3	1.4	3.6	3.6	2.9	3.9	5.6	9.1	5.4	6.9
Nb	15	19	14	5	21	18	17	16	17	13	14	16
Rb	374	377	348	395	462	423	399	457	485	420	405	468
Sn	17	13	10	6	13	11	10	13	11	7	8	7
Sr	47	36	48	15	28	31	26	32	57	61	33	43
Ta	3.4	3.1	2.2	0.8	2.4	1.9	2.2	2.6	2.1	1.1	1.3	1.4
Th	9	20	13	3	23	31	23	31	74	96	58	62
U	6	13	8	3	20	12	9	13	7	12	10	10
V	5	5	<5	<5	7	5	<5	5	18	16	9	16
W	5.9	3.4	5	0.7	4.8	3.8	2.9	3.2	3.1	1.4	2	2.4
Zr	55	96	67	22	93	105	83	105	197	246	176	196
Y	11	14	9	1	14	14	11	14	13	15	17	16
La	12.4	21.9	16.5	1.7	19.8	22.0	17.4	22.9	55.3	62.2	40.5	45.3
Ce	28.2	51.3	38.9	2.4	47.3	59.4	42.5	60.0	138	165	107	122
Pr	3.3	6.2	4.5	0.3	5.7	7.0	5.1	7.1	18.1	20.6	13.4	15.0
Nd	12.5	23.1	18.9	1.0	23.7	25.5	18.9	25.5	69.4	91.3	50.8	59.9
Sm	2.8	5.1	4.3	0.2	5.0	5.6	4.4	6.1	12.2	14.6	10.1	11.3
Eu	0.39	0.26	0.3	0.05	0.18	0.25	0.21	0.25	0.46	0.5	0.27	0.29
Gd	2.4	4.13	3.15	0.19	3.49	3.61	3.2	3.55	5.86	6.36	5.15	6.11
Tb	0.4	0.62	0.44	0.04	0.57	0.63	0.46	0.6	0.74	0.74	0.74	0.75
Dy	2.06	2.88	1.92	0.15	2.9	2.78	2.22	2.54	2.48	3.12	3.4	3.17
Ho	0.31	0.42	0.3	<.05	0.41	0.47	0.32	0.43	0.34	0.44	0.54	0.48
Er	0.81	1.07	0.64	0.13	1.15	1.14	0.83	1.09	0.88	1.05	1.42	1.28
Tm	0.11	0.15	0.09	<.05	0.15	0.15	0.16	0.16	0.15	0.13	0.2	0.18
Yb	0.67	0.93	0.54	0.17	0.98	0.93	0.7	0.83	0.87	0.93	1.37	1.05
Lu	0.08	0.09	0.07	0.02	0.12	0.13	0.11	0.1	0.13	0.13	0.13	0.15

3. Measurement of Radioactivity

Field radioactivity measurement (γ-spectrometry) was used as a method supporting to distinguish between the individual granite types. The measurement covered the whole area of the Plechý/Plöckenstein pluton, about 130 km².

Results of field measurements of uranium and thorium concentration on more than 400 locations are summarised in Text-Figs. 1 and 3. Uranium concentration is similar in all rock types, only occasionally exceeding 20 ppm. On the contrary, thorium concentration is highly variable and may serve as a sensitive rock-type indicator.

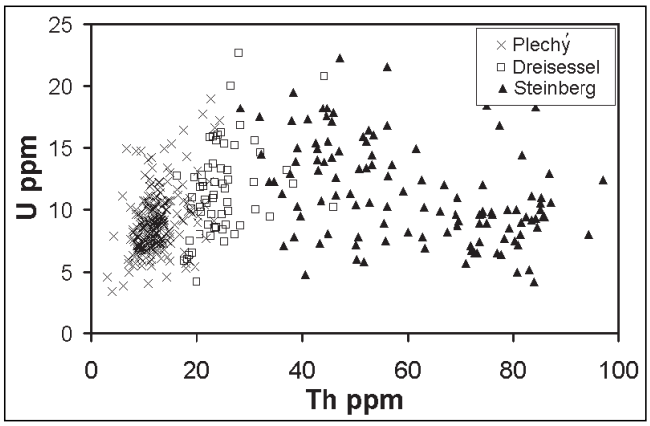

Text-Fig. 3.
Contents of U and Th in granites of the Plechý/Plöckenstein pluton according to field measurements.

4. Whole Rock Chemistry

All three granite types are peraluminous, with ASI (aluminum saturation index = molar Al_2O_3/[CaO + Na_2O + K_2O]) ranging mostly between 1.15 and 1.25. Granites of the Plechý and Dreisessel types are chemically relatively homogeneous; the composition of the Steinberg granite varies slightly. Typical chemical analyses are presented in Table 1; the variations of selected major and trace elements are shown in Figure 4.

The Plechý granite is the most silica-rich with 72–74 wt.% SiO_2, and displays low concentrations of Fe (1.2–1.7 wt.% Fe_2O_3tot), Mg (0.1–0.3 wt.% MgO), and Ca (0.5–0.6 wt.% CaO). Potassium predominates sodium (4.8–5.2 wt.% K_2O versus 3–4 wt.% Na_2O). Trace element concentrations are well comparable with the Eisgarn granite s.s. from the South Bohemian Pluton (BREITER & KOLLER, 1999), ranging between 300–400 ppm Rb, 40–80 ppm Zr, and 10–20 ppm Th.

The Dreisessel granite has a major-element concentrations nearly identical to that of the Plechý granite (Text-Fig. 4). Among trace elements, Rb, Zr, light rare-earth elements (LREE) and Zn are slightly enriched, and Y and Pb are depleted compared to the Plechý granite.

The Steinberg granite has lower silica (SiO_2 ranging from 70.5 to 72.0 wt.%, occasionally up to 74 wt.%) and Na (2.6–3.1 wt.% Na_2O), and higher Fe (1.8–2.5 wt.% Fe_2O_3tot), MgO (0.3–0.6 wt.%), CaO (0.7–1.0 wt.%), and K_2O (4.8–6.2 wt.%) compared to the other granites. The enrichment in Zr (130–220 ppm) and especially in Th (40–90 ppm) is remarkable.

The dykes cutting the Plechý granite are more siliceous and more leucocratic than the hosting granite. Trace-element concentrations are similar to the Plechý granite.

Text-Fig. 5 demonstrates correlations between titanium and some major and trace elements. TiO_2 concentration decreases during fractionation because Ti is preferentially accommodated in early crystallising Ti-oxides and biotite. In fractionated granites with similar SiO_2 content, titanium serves as a better indicator of the degree of fractional crystallisation (FÖRSTER et al., 1999)

The chondrite-normalised REE distribution patterns are in the range of other peraluminous granites and show relative enrichment of LREE (Ce/YbCN = 10-20) and a strongly negative Eu-anomaly (Fig. 6). The Steinberg granite differs from the other two granite types in having higher LREE concentrations due to the high amount of monazite.

5. Mineral Composition

5.1. Feldspars

Both feldspars from all three granite types are chemically close to end-member composition (Text-Fig. 7). K-feldspar contains usually 3–7 mol% albite component, with no visible core-to-rim zonation. The concentration of P_2O_5 increases from the core to the rim from 0.3 wt.% up to about 0.5 wt.%. In slightly altered samples, phosphorous concentration in feldspar rims decreases. Barium concentration is low, usually below 0.1 wt. %. Only in the Steinberg granite, BaO concentration occasionally approaches 0.4 wt.%.

Plagioclase is generally albite, only some feldspar cores in the Steinberg granite are oligoclase in composition. Content and distribution of phosphorus are analogous to what has been established in K-feldspars.

5.2. Micas

In all three granites, the Mg/(Fe+Mg) ratios are similar in biotite (0.2-0.3) and muscovite (0.35-0.55, Tables 2 & 3, Fig. 8). Plechý biotites have higher Al^{IV} and Plechý muscovites higher Al^{VI} than micas from the porphyritic granites. The behaviour of titanium is remarkable: this element tends to be most enriched in biotites from the Plechý granite, but muscovites from this granite are the most Ti-poor (Text-Fig. 9). The distribution coefficient of titanium between biotite and muscovite increases from about 2 in the Steinberg granite to about 6 in the Plechý granite. A similar evolution of this distribution coefficient was mentioned by SIEBEL (1993) from the Leuchtenberg granite: it increases from 4–5 in less fractionated granites to 12–17 in strongly fractionated granites. Thus, it seems likely that the distribution coefficient changes during fractional crystallisation and that in more fractionated rocks, biotite tends to incorporate more Ti compared to muscovite.

In terms of trace elements (Table 4), the micas from all three granites are similar. Variability in each granite is larger than the differences among granite types.

5.3. Apatite

Apatite is the most common accessory mineral in all three granites. It forms short prismatic, subhedral to anhedral crystals, mainly hosted in biotite. Its chemical composition is variable (Table 5), with slightly higher Mn/Fe and Y/Ce ratios in the Plechý granite in comparison to the porphyritic granites.

5.4. Zircon

Zircon from the Steinberg granite forms homogeneous crystals, which are relatively poor in trace elements, close to ideal $ZrSiO_4$. Zircon from the Dreisessel granite is slightly enriched in U, Sc, P, and Y (Table 6, Text-Fig. 11), but is otherwise similar to those from the Steinberg granite. Zircon grains from the Plechý granite are distinctly zoned and often contain metamict zones, enriched in U (1–3 wt.%

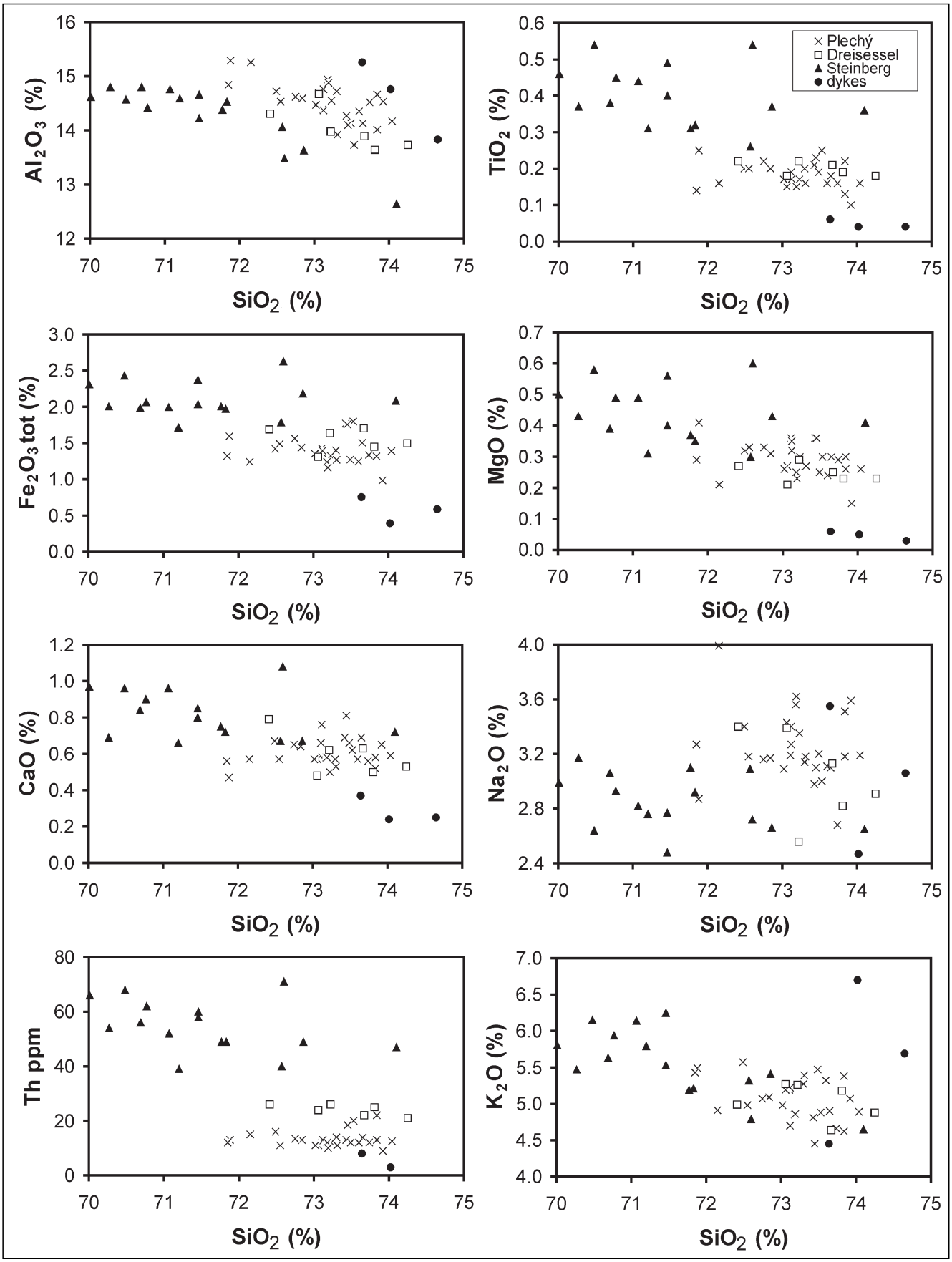

Text-Fig. 4.
Harker diagrams of granites of the Plechý/Plöckenstein pluton.

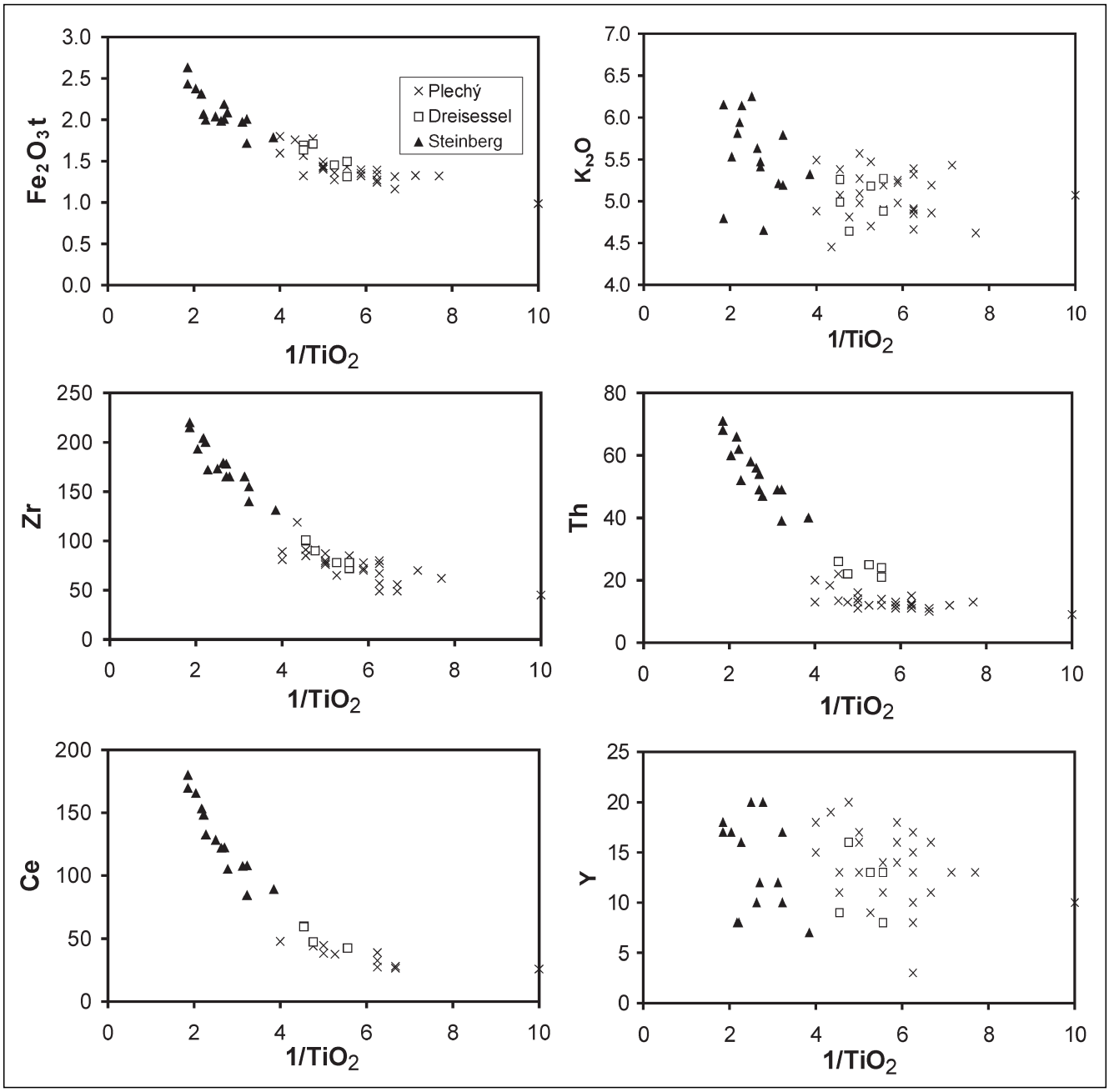

Text-Fig. 5.
Major and trace element versus $1/TiO_2$ diagrams showing compositional evolution of granites during fractional crystallisation.

UO_2), P (1.0–1.5 wt.% P_2O_5), Sc (0.15–0.35 wt.% Sc_2O_3), and Y (1–2 wt.% Y_2O_3). The concentration of HfO_2 is similar, in all granites varying around 1.5 wt.%. The Zr/Hf-atomic ratio is 60–70 in zircon from the Plechý granite and 70-80 in zircon from the porphyritic granites.

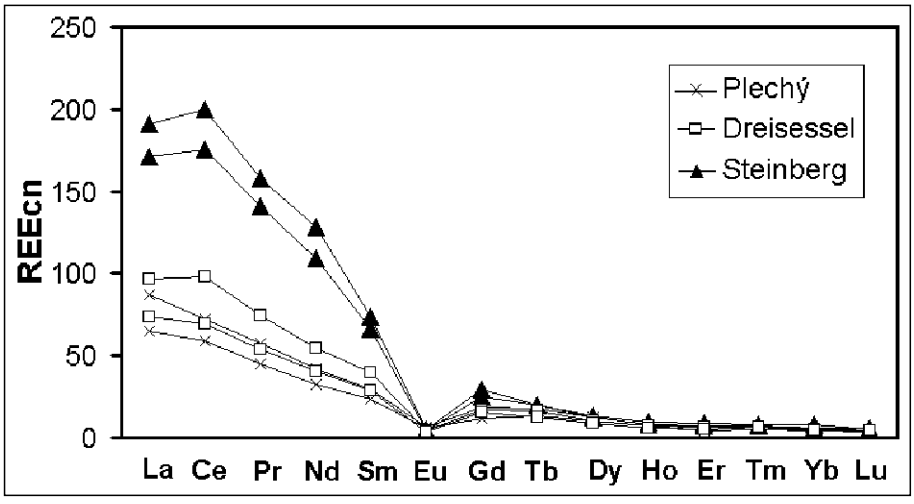

Text-Fig. 6.
Chondrite-normalised distribution of REE in typical samples of the Plechý/Plöckenstein pluton.

Table 2.
Chemical composition (wt. %) and empirical formulae (based on 44 positive charges) of biotite (WDS-microprobe analyses, CAMECA SX100, Geological Institute, Academy of Science of Czech Republic, Praha).

Rock	Plechý granite			Dreisessel granite			Steinberg granite		
Sample	4368	3625	3623	4365	3707	4363	4139	4271	3698
SiO_2	34.48	34.05	34.36	34.94	34.31	34.50	34.52	35.66	35.44
TiO_2	2.37	2.75	2.81	1.93	2.49	2.35	2.50	2.28	2.39
$A_{l2}O_3$	18.44	18.85	18.72	18.13	18.53	18.41	17.74	16.94	17.60
FeO	26.75	24.50	25.22	27.44	27.67	27.16	25.18	24.72	23.12
MgO	3.46	4.86	3.97	3.13	2.75	3.56	5.27	6.40	5.97
MnO	0.40	0.42	0.38	0.19	0.38	0.21	0.24	0.14	0.09
CaO	0.00	0.00	0.03	0.04	0.00	0.00	0.01	0.01	0.00
BaO	0.00	0.00	0.00	0.00	0.07	0.00	0.00	0.00	0.04
Na_2O	0.07	0.04	0.10	0.04	0.11	0.09	0.09	0.07	0.06
K_2O	9.76	9.78	9.46	9.55	9.56	9.69	9.44	9.83	9.85
Total	95.75	95.25	95.07	95.40	95.87	95.96	95.00	96.05	94.55
Si	5.446	5.354	5.418	5.539	5.433	5.440	5.448	5.549	5.559
Ti	0.282	0.325	0.333	0.230	0.297	0.279	0.297	0.267	0.281
Al	3.433	3.493	3.478	3.387	3.459	3.420	3.299	3.107	3.2534
Fe	3.533	3.221	3.325	3.638	3.664	3.581	3.323	3.217	3.033
Mg	0.815	1.140	0.933	0.741	0.650	0.836	1.239	1.484	1.396
Mn	0.054	0.055	0.050	0.025	0.051	0.028	0.032	0.018	0.012
Ca	0.000	0.000	0.005	0.007	0.000	0.000	0.002	0.001	0.000
Ba	0.000	0.000	0.000	0.000	0.004	0.000	0.000	0.000	0.003
Na	0.022	0.013	0.031	0.012	0.032	0.026	0.028	0.022	0.017
K	1.967	1.960	1.902	1.932	1.932	1.950	1.901	1.952	1.971
Mg/(Mg+Fe)	0.187	0.261	0.219	0.170	0.151	0.189	0.272	0.316	0.315
Al^{VI}	0.878	0.847	0.896	0.925	0.892	0.860	0.747	0.656	0.814
Al^{IV}	2.554	2.646	2.582	2.461	2.567	2.560	2.552	2.451	2.441

Table 3.
Chemical composition (wt. %) and empirical formulae (based on 44 positive charges) of muscovite (WDS-microprobe analyses, CAMECA SX100, Geological Institute, Academy of Science of Czech Republic, Praha).

Rock	Plechý granite			Dreisessel granite			Steinberg granite		
Sample	3625	3623	2283	4365	4363	3707	4139	4271	4362
SiO_2	46.43	46.35	46.52	46.37	46.09	46.26	46.21	47.35	46.36
TiO_2	0.59	0.56	0.59	0.75	0.73	0.70	1.01	1.22	0.97
Al_2O_3	35.45	34.40	35.05	33.53	32.38	34.04	33.15	32.73	33.42
FeO	1.52	1.86	1.29	2.08	2.72	1.92	1.93	2.55	2.22
MgO	0.86	0.92	0.70	0.96	1.08	0.87	1.13	1.57	0.97
MnO	0.03	0.05	0.00	0.00	0.00	0.03	0.08	0.00	0.03
CaO	0.01	0.00	0.02	0.00	0.00	0.03	0.00	0.00	0.00
BaO	0.02	0.00	0.02	0.01	0.10	0.00	0.02	0.00	0.12
Na_2O	0.53	0.65	0.65	0.77	0.41	0.82	0.66	0.31	0.84
K_2O	10.22	10.26	10.17	10.50	11.04	10.62	10.28	9.82	10.43
Total	95.59	95.00	94.96	94.95	94.52	95.26	94.45	95.55	95.34
Si	6.152	6.199	6.197	6.230	6.264	6.195	6.233	6.297	6.215
Ti	0.059	0.056	0.059	0.076	0.074	0.070	0.102	0.122	0.098
Al	5.535	5.422	5.503	5.308	5.186	5.373	5.269	5.129	5.280
Fe	0.169	0.208	0.144	0.234	0.309	0.215	0.218	0.284	0.249
Mg	0.170	0.183	0.138	0.192	0.219	0.173	0.228	0.311	0.194
Mn	0.003	0.006	0.000	0.000	0.000	0.003	0.009	0.000	0.004
Ca	0.002	0.000	0.003	0.000	0.000	0.005	0.000	0.000	0.000
Ba	0.001	0.000	0.001	0.000	0.005	0.000	0.001	0.000	0.006
Na	0.135	0.170	0.168	0.201	0.107	0.214	0.174	0.079	0.218
K	1.727	1.751	1.728	1.801	1.914	1.813	1.768	1.666	1.784
Mg/(Mg+Fe)	0.502	0.468	0.489	0.451	0.415	0.446	0.511	0.523	0.437
Al^{VI}	3.688	3.621	3.699	3.535	3.450	3.567	3.502	3.426	3.495
Al^{IV}	1.848	1.801	1.803	1.772	1.736	1.805	1.767	1.703	1.785

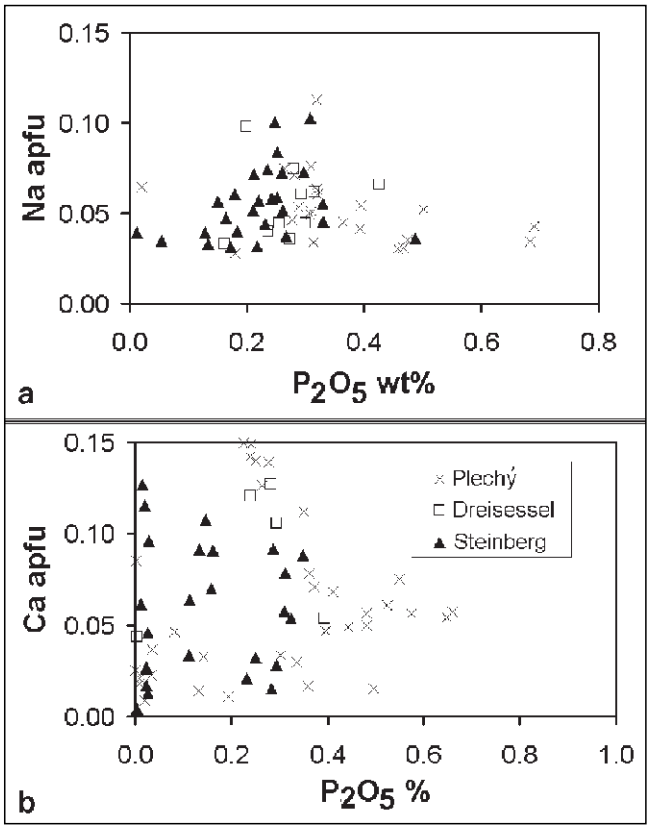

Text-Fig. 7.
a) Contents of Na and P in K-feldspars.
b) Variation of Ca versus P concentration in plagioclase (apfu = atoms per formula unit).

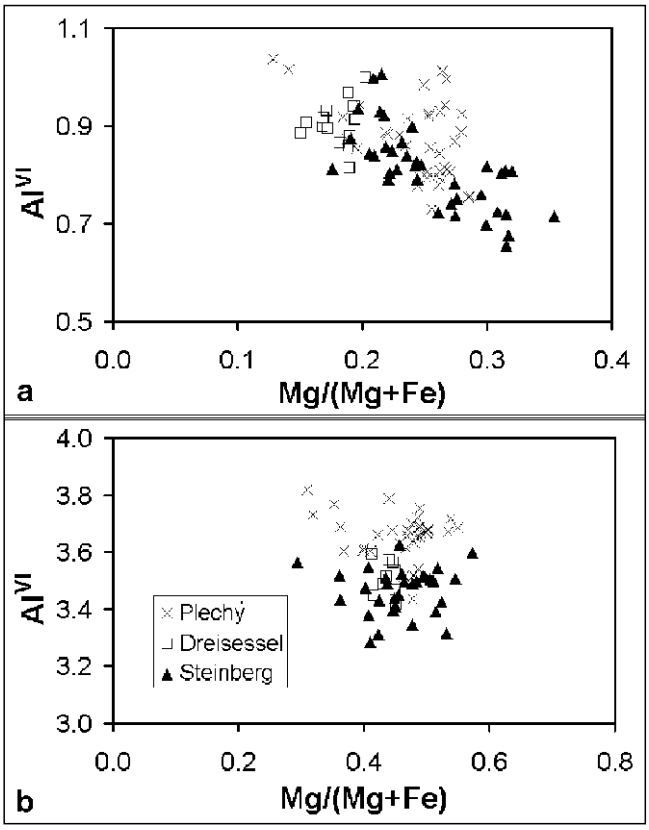

Text-Fig. 8.
Chemical composition of biotite (a) and muscovite (b).
Mg/(Mg+Fe) versus Al in octahedral position.

5.5. Monazite

Monazite from the Plechý granite is enriched in U, Y, and Si and depleted in Th compared to monazite from the Steinberg granite. Whereas in the monazite from the Plechý granite, Th is incorporated according to the Th+Ca↔2 REE (cheralite) substitution, monazite from the Steinberg granite contains substantial $ThSiO_4$ (huttonite) component (Table 7, Text-Fig. 12).

Monazite from the Dreisessel granite is chemically intermediate between both previous granite types.

Table 4.
Contents of trace elements in micas (F in wt.% by ion-selective electrode, other elements in ppm by AAS), analysed in monomineralic concentrates, laboratory of CGS Praha.

Rock		Sample	F	Li	Rb	Cs	Be	Ba	Zn	Pb	V
Steinberg granite	Mu	4139	1.17	327	970	19	20.6	207	143	17	73
		4271	n.a.	350	690	20	21.5	270	158	23	66
		4272	0.99	383	2030	15	24.4	162	168	10	79
		4278	1.42	490	1110	13	27.4	63	197	<10	44
		4362	1.11	420	1070	28	16.5	72	145	<10	50
		4369	0.99	411	1080	32	16.6	81	167	22	50
Dreisessel granite	Mu	4366	1.17	579	1270	62	26.1	81	211	<10	50
		4367	1.09	593	1240	77	23.8	63	181	<10	40
		4365	1.14	677	1330	76	26.3	81	187	<10	29
		4370	0.89	504	1180	35	13.1	54	132	12	22
Steinberg granite	Bi	4271	1.67	705	1650	135	14.7	396	1166	19	72
		4272	1.96	845	1650	108	6.5	522	1310	17	49
		4278	2.40	976	1510	66	5.5	621	1487	11	61
		4362	1.77	962	1750	131	4.9	171	1375	<10	52
		4369	1.99	929	1780	108	4.3	270	1230	<10	68
		4366	1.93	733	2020	269	6.5	225	1404	15	54
		4367	1.89	1242	1950	337	7.3	180	1390	14	41
Dreisessel granite	Bi	4365	1.89	1312	2100	346	7.0	117	1430	10	19
		4370	1.64	1406	2030	249	5.0	108	1403	16	21
Plechý granite	Bi	4368	1.02	1284	1530	207	4.9	63	1373	20	50
		4277	0.84	1284	1470	219	4.7	81	1066	<10	55

Rock	Plechý granite			Dreisessel granite			Steinberg granite		
Sample	3854	2034	3625	4363	4363	4365	4367	4362	4139
F	3.67	3.93	3.72	3.78	4.76	4.48	3.36	4.31	3.63
Cl	0.03	0.00	0.02	0.02	0.00	0.01	0.01	0.00	0.05
P_2O_5	42.53	40.63	41.42	42.70	41.22	41.02	42.17	42.77	41.46
CaO	54.20	52.96	51.82	55.53	54.67	53.71	53.32	55.52	54.38
MnO	1.04	1.29	1.96	0.15	0.68	1.05	1.05	0.10	0.46
FeO	0.24	0.44	0.84	0.03	0.40	0.28	0.67	0.10	0.26
Na_2O	0.19	0.16	0.22	0.13	0.17	0.14	0.16	0.12	0.21
SiO_2	0.00	0.03	0.03	0.02	0.02	0.01	0.03	0.01	0.02
SrO	0.01	0.01	0.00	0.00	0.00	0.00	0.00	0.00	0.02
Y_2O_3	0.27	0.29	0.27	0.11	0.22	0.13	0.21	0.13	0.17
ThO_2	0.01	0.00	0.01	0.01	0.00	0.01	0.01	0.02	0.01
UO_2	0.04	0.00	0.00	0.01	0.00	0.02	0.03	0.00	0.03
Ce_2O_3	0.09	0.10	0.08	0.09	0.13	0.14	0.19	0.08	0.16
Total	102.32	99.88	100.42	102.59	102.27	101.02	101.21	103.20	100.86
F	0.969	1	1	0.995	1	1	0.895	1	0.975
Cl	0.004	0.000	0.003	0.002	0.000	0.001	0.001	0.000	0.007
P	3.008	2.971	3.001	3.006	2.964	2.977	3.009	3.008	2.982
Ca	4.851	4.902	4.751	4.947	4.975	4.932	4.814	4.942	4.950
Mn	0.074	0.094	0.142	0.010	0.049	0.076	0.075	0.007	0.033
Fe	0.017	0.032	0.060	0.002	0.029	0.020	0.047	0.007	0.019
Na	0.031	0.026	0.036	0.021	0.028	0.024	0.025	0.019	0.034
Si	0.000	0.003	0.002	0.002	0.001	0.001	0.003	0.001	0.002
Sr	0.000	0.000	0.000	0.000	0.000	0.000	0.000	0.000	0.001
Y	0.012	0.013	0.012	0.005	0.010	0.006	0.009	0.006	0.008
Th	0.000	0.000	0.000	0.000	0.000	0.000	0.000	0.000	0.000
U	0.001	0.000	0.000	0.000	0.000	0.000	0.000	0.000	0.001
Ce	0.003	0.003	0.002	0.003	0.004	0.004	0.006	0.002	0.005

Table 5.
Chemical composition (wt.%) and empirical formulae (based on 25 positive charges) of apatite. (WDS-microprobe analyses, CAMECA SX100, Masaryk University and Czech Geological Survey Brno). Rem.: Result of fluorine measurement depends on the orientation of analysed apatite crystal. Theoretical F-content in pure fluorapatite is 3.77 wt.%. Where we analysed higher than maximal possible F-content, we put to the formula F (apfu) = 1.

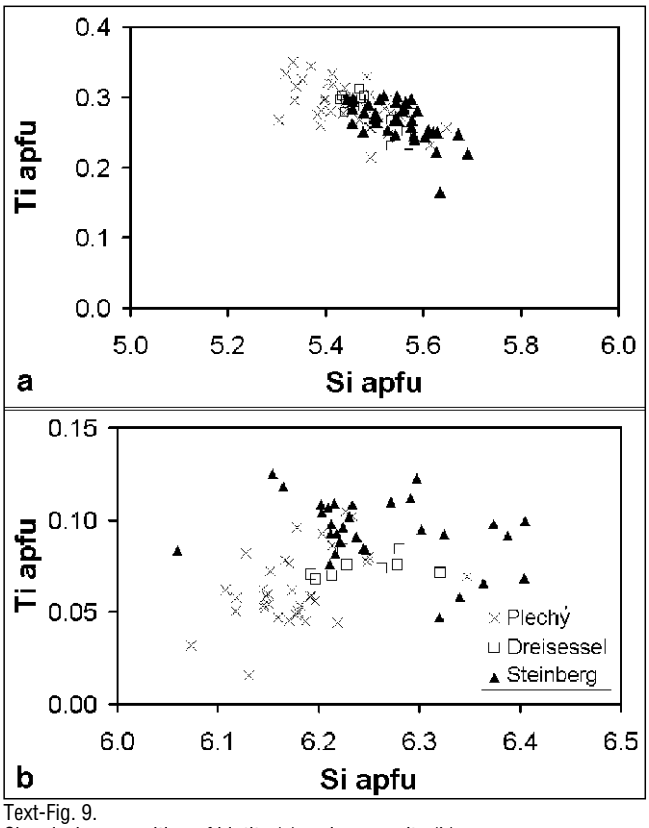

Text-Fig. 9.
Chemical composition of biotite (a) and muscovite (b).
Contents of Si versus Ti.

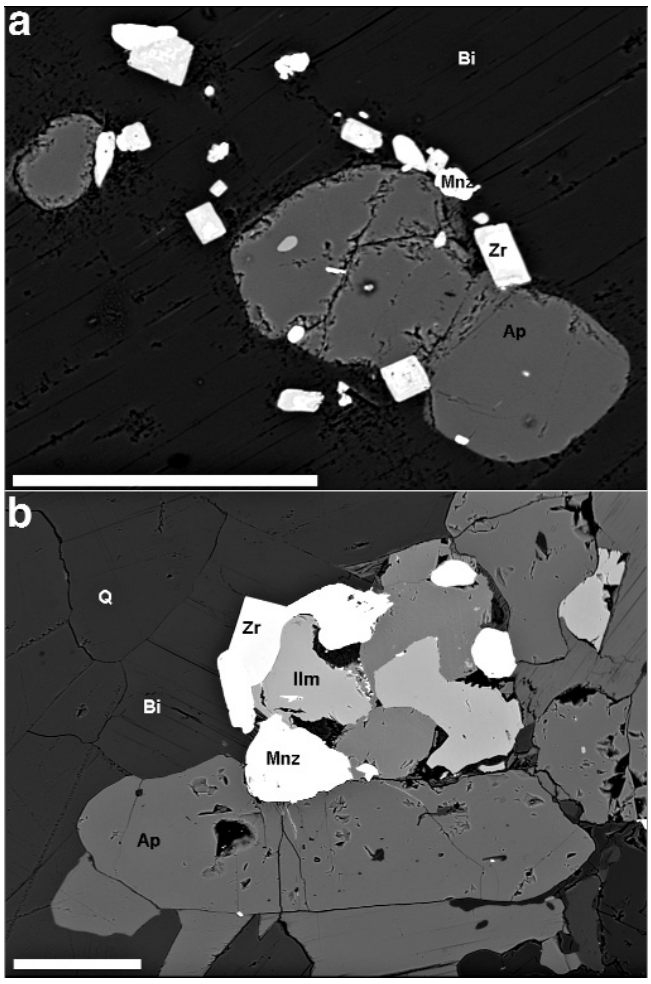

Text-Fig. 10.
Typical associations of accessory minerals.
a) Plechý granite (monazite (white) and zoned zircon around apatite crystal, all hosted in biotite.
b) Steinberg granite (monazite, homogeneous zircon, ilmenite and apatite hosted in biotite).
Scale bars 100 m.

Granite	Plechý granite				Dreisessel granite			Steinberg granite		
Sample	2283	2283	3623	3623	4363	4363	3619	4139	3859	4367
P_2O_5	**2.40**	1.33	1.82	0.41	0.25	0.58	0.15	0.73	1.62	0.55
SiO_2	*25.36*	26.52	27.06	31.38	31.70	29.94	32.32	31.00	26.32	31.25
ZrO_2	*50.31*	55.27	56.63	64.06	64.42	60.03	65.45	62.75	54.19	62.72
HfO_2	1.22	1.53	1.43	1.49	1.37	1.53	1.45	1.30	1.03	**1.81**
ThO_2	0.08	0.00	0.08	0.02	0.02	0.05	0.00	0.01	**0.53**	0.00
UO_2	4.82	1.78	1.38	0.41	0.10	0.97	0.16	0.71	2.36	1.00
Al_2O_3	0.30	0.30	**0.43**	0.02	0.06	0.09	0.01	0.03	0.04	0.01
Y_2O_3	**2.54**	1.07	0.80	0.21	0.14	0.56	0.13	0.57	**1.84**	0.36
Yb_2O_3	**0.41**	0.21	0.16	0.03	0.00	0.14	0.03	0.14	**0.32**	0.10
Sc_2O_3	0.25	0.25	0.17	0.06	0.05	0.10	0.02	0.14	0.18	0.14
FeO	0.45	0.57	**1.29**	0.94	0.07	0.25	0.11	0.54	0.50	0.12
MnO	0.36	**0.46**	0.08	0.01	0.01	0.08	0.00	0.00	**0.47**	0.01
CaO	1.96	**2.39**	**2.25**	0.04	0.05	0.37	0.00	0.02	**2.36**	0.02
F	**0.43**	0.31	**0.50**	0.00	0.00	0.02	0.00	0.00	**0.32**	0.00
Total	90.87	92.00	94.05	99.05	98.27	94.87	99.83	97.94	92.09	98.32
P	0.072	0.039	0.052	0.011	0.007	0.016	0.004	0.020	0.047	0.015
Si	0.897	0.913	0.909	0.979	0.992	0.979	0.995	0.976	0.908	0.984
Zr	0.868	0.928	0.927	0.975	0.983	0.958	0.983	0.964	0.911	0.964
Hf	0.012	0.015	0.014	0.013	0.012	0.014	0.013	0.012	0.010	0.016
Th	0.001	0.000	0.001	0.000	0.000	0.000	0.000	0.000	0.004	0.000
U	0.038	0.014	0.010	0.003	0.001	0.007	0.001	0.005	0.018	0.007
Al	0.013	0.012	0.017	0.001	0.002	0.003	0.000	0.001	0.002	0.001
Y	0.048	0.020	0.014	0.003	0.002	0.010	0.002	0.009	0.034	0.006
Yb	0.004	0.002	0.002	0.000	0.000	0.001	0.000	0.001	0.003	0.001
Sc	0.008	0.008	0.005	0.001	0.001	0.003	0.001	0.004	0.005	0.004
Fe	0.013	0.016	0.036	0.025	0.002	0.007	0.003	0.014	0.014	0.003
Mn	0.011	0.013	0.002	0.000	0.000	0.002	0.000	0.000	0.014	0.000
Ca	0.074	0.088	0.081	0.001	0.002	0.013	0.000	0.001	0.087	0.001
F	0.048	0.034	0.053	0.000	0.000	0.002	0.000	0.000	0.035	0.000
Zr/Hf	70	62	68	74	80	67	77	82	90	59

Table 6.
Chemical composition (wt.%) and empirical formulae (based on 8 positive charges) of zircon. (WDS-microprobe analyses, CAMECA SX100, Masaryk University and Czech Geological Survey, Brno).

5.6. Rutile and Ilmenite

Rutile is present as an accessory phase in all granite types. The chemical composition of rutile is similar in all granites. Nb_2O_5 and /or FeO (0.1–0.4 wt%) are the only non-formula elements detected by EMPA (Text-Fig. 13). Manganese, Mg, Cr, and V concentrations are generally below their detection limits. Ilmenite is the most common Ti-bearing phase beside biotite. In the Steinberg granite, ilmenite forms a chemically homogeneous population with 2–4 wt% MnO_2 and 0.10–0.15 wt.% Nb_2O_5. Ilmenite from the Plechý and Dreisessel granites shows a large variation of Mn and is slightly Nb-enriched. The contents of Mg, Al, Si, V, Cr, Sn, and Ta are usually below the detection limits of the microprobe (Table 8).

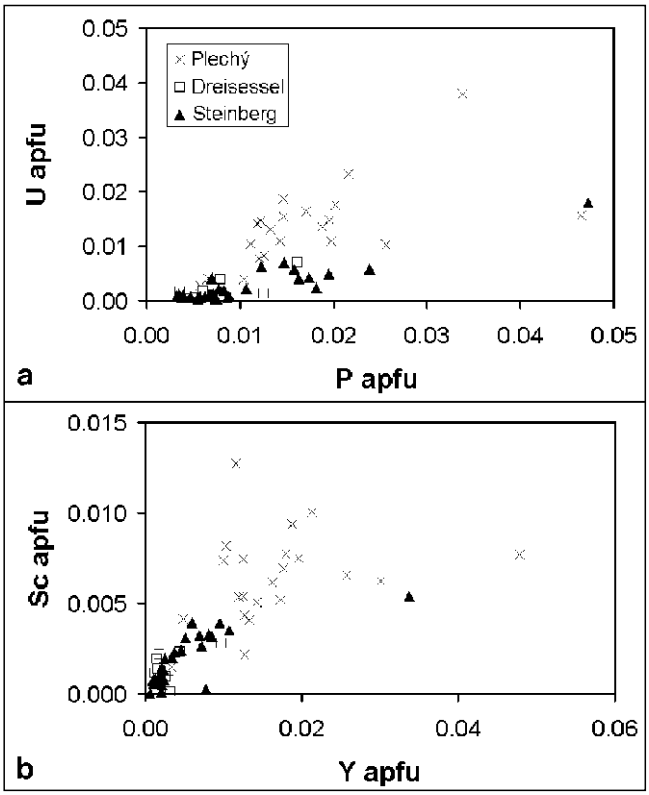

Text-Fig. 11.
a) Plot of uranium versus phosphorus concentration in zircon.
b) Plot of scandium versus yttrium concentration in zircon.

Granite	Plechý granite				Dreisessel granite			Steinberg granite			
Sample	2283	2283	3623	3623	4363	4363	4365	4278	4278	3619	3619
P_2O_5	30.09	30.17	29.28	28.76	23.38	27.82	27.58	29.14	28.71	27.70	28.94
SiO_2	0.44	0.31	0.30	0.36	**3.74**	0.42	0.91	0.76	1.08	1.07	0.77
ThO_2	12.53	9.44	12.36	7.86	**14.69**	11.01	8.90	**16.99**	**28.47**	13.38	**16.34**
UO_2	1.37	**3.18**	**2.62**	0.45	1.00	2.16	0.21	0.73	1.37	0.31	0.61
Al_2O_3	0.00	0.00	0.00	0.00	1.03	0.01	0.00	0.01	0.00	0.00	0.01
La_2O_3	9.56	9.26	10.06	12.81	11.37	10.19	13.50	7.60	8.64	9.25	7.83
Ce_2O_3	24.03	22.97	22.95	27.65	23.58	24.11	29.93	21.87	*18.50*	25.31	22.66
Pr_2O_3	2.94	2.72	2.52	3.01	2.39	2.76	3.08	3.04	1.84	3.36	2.90
Nd_2O_3	11.09	10.54	9.24	11.35	7.59	9.96	10.65	11.74	5.66	13.47	11.93
Sm_2O_3	2.32	2.73	2.19	2.10	1.36	2.13	1.75	2.44	0.88	1.95	2.45
Gd_2O_3	1.09	1.89	1.50	1.11	0.59	1.24	0.51	1.17	0.29	0.65	1.22
Dy_2O_3	0.39	0.78	0.68	0.34	0.19	0.55	0.06	0.44	0.10	0.14	0.38
Er_2O_3	0.09	0.12	0.11	0.06	0.04	0.09	0.00	0.08	0.03	0.00	0.08
Y_2O_3	1.18	**2.11**	**1.92**	0.83	0.48	1.75	0.21	1.24	0.39	0.24	1.10
PbO	0.24	0.29	0.29	0.13	0.24	0.25	0.13	0.26	0.45	0.18	0.25
CaO	2.75	2.68	2.98	1.51	2.29	2.73	1.14	3.02	**5.31**	2.02	2.93
Total	100.11	99.19	99.04	98.34	93.99	97.26	98.62	100.52	101.71	99.02	100.38
P	0.991	0.997	0.982	0.979	0.838	0.963	0.951	0.969	0.951	0.949	0.966
Si	0.017	0.012	0.012	0.014	0.158	0.017	0.037	0.030	0.042	0.043	0.030
Th	0.111	0.084	0.111	0.072	0.141	0.102	0.082	0.152	0.253	0.123	0.147
U	0.012	0.028	0.023	0.004	0.009	0.020	0.002	0.006	0.012	0.003	0.005
Al	0.000	0.000	0.000	0.000	0.051	0.001	0.000	0.000	0.000	0.000	0.000
La	0.137	0.133	0.147	0.190	0.177	0.154	0.203	0.110	0.125	0.138	0.114
Ce	0.342	0.328	0.333	0.407	0.365	0.361	0.446	0.315	0.265	0.375	0.327
Pr	0.042	0.039	0.036	0.044	0.037	0.041	0.046	0.043	0.026	0.050	0.042
Nd	0.154	0.147	0.131	0.163	0.115	0.145	0.155	0.165	0.079	0.195	0.168
Sm	0.031	0.037	0.030	0.029	0.020	0.030	0.025	0.033	0.012	0.027	0.033
Gd	0.014	0.024	0.020	0.015	0.008	0.017	0.007	0.015	0.004	0.009	0.016
Dy	0.005	0.010	0.009	0.004	0.003	0.007	0.001	0.006	0.001	0.002	0.005
Er	0.001	0.001	0.001	0.001	0.001	0.001	0.000	0.001	0.000	0.000	0.001
Y	0.024	0.044	0.041	0.018	0.011	0.038	0.004	0.026	0.008	0.005	0.023
Pb	0.002	0.003	0.003	0.001	0.003	0.003	0.001	0.003	0.005	0.002	0.003
Ca	0.115	0.112	0.127	0.065	0.104	0.120	0.050	0.127	0.223	0.088	0.124

Table 7.
Chemical composition (wt. %) and empirical formulae (based on 8 positive charges) of monazite. (WDS-EMPA analyses, CAMECA SX100, MU and Czech Geological Survey, Brno).

6. Geochronology

Mineral age-dating was undertaken to better constrain the crystallisation and cooling history of the Plechý-Plöckenstein pluton (Table 9).

The $^{207}Pb/^{206}Pb$ single-zircon evaporation ages from all three granite types fall in short time interval between 328 and 325 Ma (W. Siebel et al., in prep) giving the probable age of crystallisation.

The mica ages show a relatively large scatter. Ar-Ar plateau ages of muscovites are the same or, on average, only slightly older (318–313 Ma) than total gas ages of

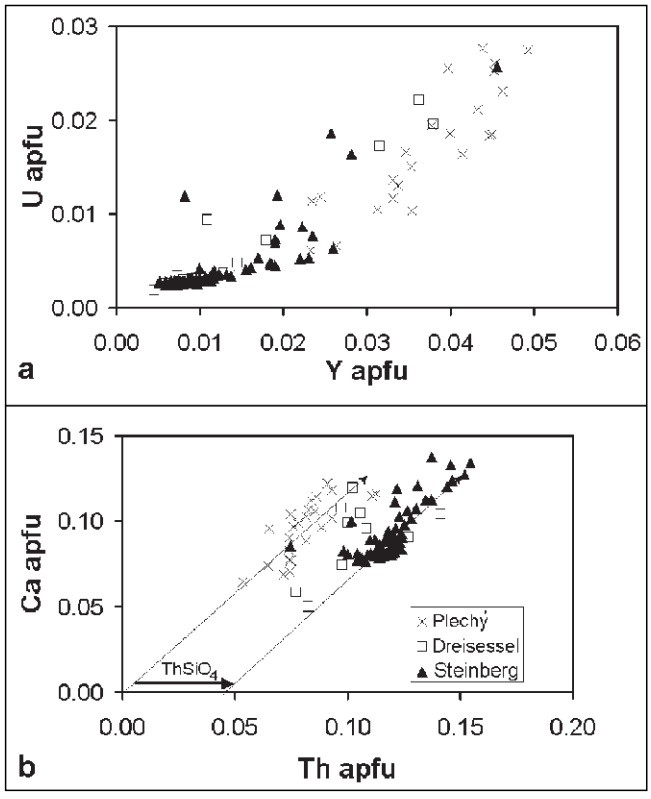

Text-Fig. 12.
Chemical composition of monazite.
a) contents of Y versus U.
b) Th versus Ca (all in atoms per formula unit).
Thin arrows demonstrate the Ca+Th↔2REE (cheralite) substitution; bold arrow shows the $ThSiO_4$↔REEPO4 (hutonite) substitution. Monazite from the Steinberg granite contains about 4 mol.% of hutonite.

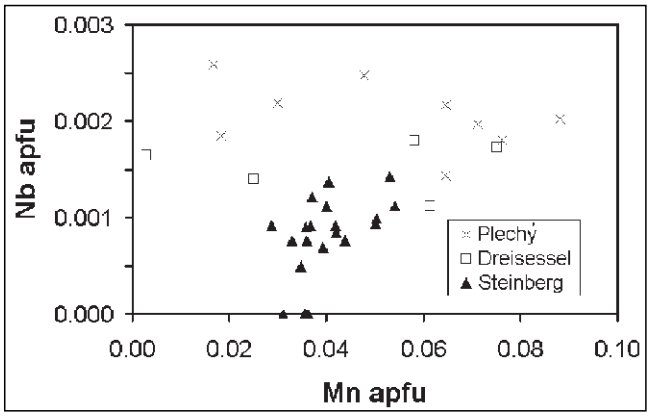

Text-Fig. 13.
Chemical composition of ilmenite.

biotites (313–311 Ma). There are no differences in Ar-Ar ages between the Plechý and Dreisessel granite types (see Table 9 and Text-Fig. 14), whereas the sample from the Steinberg granite yields slightly lower muscovite and biotite ages.

Rb-Sr dating of micas suggest a disturbed cooling of the pluton. The Rb-Sr muscovite dates for the granites largely correspond, within error limit, with the Ar-Ar muscovite dates: With one exception, the ages fall between 324±4 and 315±4 Ma (2σ error). A muscovite from the Plechý granite, however, yields a younger Rb-Sr date of 306±4 Ma. The three Rb-Sr biotite dates vary largely from 327±4 Ma, through 314±4 Ma to 289±4 Ma.

U-Th-Pb microprobe ages of monazite from the Plechý granite and the Steinberg granite are largely consistent with the Ar-Ar and Rb-Sr mica ages whereas the age obtained for two monazite populations of the Dreisessel granite are in accordance with the single-zircon evaporation ages.

Sr-isotope data of whole rock samples are listed in Table 10. Each of the three granite varieties has distinct trace element characteristics with respect to Rb and Sr (see also Table 1). The sample analysed from the Dreisessel granite has a higher Rb and lower Sr concentration, and that from the Steinberg granite has a higher Rb and higher Sr concentration than the four investigated samples from the Plechý granite. The best-fit regression line in the Sr-isotope evolution diagram points to an age of 318 Ma (only orientational 3-sample regression), a value that is in agreement with the muscovite cooling-age. Initial $^{87}Sr/^{86}Sr$ ratios are between 0.711–0.714 for all three granite types.

7. Discussion

7.1. Cooling History of the Pluton

The variation in Ar-Ar and namely Rb-Sr mica-ages is obvious. The exact reason for the relatively large age spread is unknown, it could be that the Plechý-Plöckenstein pluton was deeply buried and parts of it remained at temperatures above the closure temperature for muscovite

Table 8.
Chemical composition (wt. %) and empirical formulae of Ti-oxides (WDS-EMPA analyses, CAMECA SX100, MU and Czech Geological Survey, Brno).

Mineral	Ilmenite										Rutile				
Rock	Plechý granite				Dreisessel granite		Steinberg granite				Plechý granite	Dreisessel granite		Steinberg granite	
Sample	3854	2034	3623	3625	4365	4365	3619	4271	4362	4139	2283	4363	4365	4367	4271
TiO_2	55.70	52.08	51.87	54.97	52.69	54.88	57.63	52.85	53.02	54.26	99.53	98.86	93.95	97.28	98.98
ZrO_2	0.00	0.00	0.00	0.00	0.00	0.00	0.00	0.00	0.00	0.00	0.00	0.00	0.00	0.00	0.00
SiO_2	0.01	0.05	0.13	0.02	n.a.	n.a.	0.04	0.01	n.a.	0.00	0.07	n.a.	n.a.	n.a.	0.02
SnO_2	0.00	0.02	0.00	0.02	0.00	0.00	0.00	0.00	0.00	0.00	0.00	0.00	0.06	0.04	0.00
Nb_2O_5	0.24	0.26	0.29	0.32	0.22	0.18	0.07	0.10	0.15	0.16	0.34	0.34	0.50	0.13	0.22
Ta_2O_5	0.03	0.03	0.01	0.04	0.02	0.03	0.00	0.00	0.01	0.05	0.03	0.02	0.02	0.03	0.00
Al_2O_3	0.01	0.00	0.01	0.03	n.a.	n.a.	0.01	0.00	n.a.	0.01	0.07	n.a.	n.a.	n.a.	0.02
V_2O_3	0.00	0.08	0.00	0.00	0.18	0.00	0.05	0.00	0.00	0.16	0.00	0.00	0.00	0.00	0.00
Cr_2O_3	0.02	0.00	0.00	0.00	0.02	0.00	0.01	0.01	0.01	0.00	0.01	0.01	0.00	0.00	0.02
Y_2O_3	n.a.	0.02	0.00	0.00	0.01	0.00	n.a.	n.a.	0.00	n.a.	n.a.	0.03	0.00	0.00	n.a.
FeO	37.66	39.20	44.09	38.67	37.45	37.12	39.56	44.54	42.12	41.52	0.10	0.20	2.02	0.89	0.11
MnO	5.41	6.07	2.08	3.34	5.33	1.78	2.51	2.31	3.79	2.60	0.01	0.00	0.04	0.00	0.01
MgO	0.00	0.00	0.04	0.03	0.00	0.00	0.00	0.02	0.03	0.00	0.00	0.00	0.00	0.01	0.00
CaO	0.01	0.03	0.03	0.00	0.55	0.06	0.07	0.00	0.00	0.00	0.01	0.03	0.05	0.03	0.00
Total	99.10	97.86	98.54	97.44	96.47	94.06	99.94	99.84	99.13	98.75	100.19	99.49	96.63	98.40	99.38
Ti	1.045	1.006	0.997	1.048	1.023	1.073	1.064	1.003	1.010	1.029	0.995	0.996	0.983	0.993	0.997
Zr	0.000	0.000	0.000	0.000	0.000	0.000	0.000	0.000	0.000	0.000	0.000	0.000	0.000	0.000	0.000
Si	0.000	0.001	0.003	0.001	0.000	0.000	0.001	0.000	0.000	0.000	0.001	0.000	0.000	0.000	0.000
Sn	0.000	0.000	0.000	0.000	0.000	0.000	0.000	0.000	0.000	0.000	0.000	0.000	0.000	0.000	0.000
Nb	0.003	0.003	0.003	0.004	0.003	0.002	0.001	0.001	0.002	0.002	0.002	0.002	0.003	0.001	0.001
Ta	0.000	0.000	0.000	0.000	0.000	0.000	0.000	0.000	0.000	0.000	0.000	0.000	0.000	0.000	0.000
Al	0.000	0.000	0.000	0.001	0.000	0.000	0.000	0.000	0.000	0.000	0.001	0.000	0.000	0.000	0.000
V	0.000	0.001	0.000	0.000	0.003	0.000	0.001	0.000	0.000	0.003	0.000	0.000	0.000	0.000	0.000
Cr	0.000	0.000	0.000	0.000	0.000	0.000	0.000	0.000	0.000	0.000	0.000	0.000	0.000	0.000	0.000
Y	0.000	0.000	0.000	0.000	0.000	0.000	0.000	0.000	0.000	0.000	0.000	0.000	0.000	0.000	0.000
Fe	0.786	0.842	0.943	0.819	0.809	0.807	0.812	0.940	0.892	0.876	0.001	0.002	0.023	0.010	0.001
Mn	0.114	0.132	0.045	0.072	0.117	0.039	0.052	0.049	0.081	0.056	0.000	0.000	0.000	0.000	0.000
Mg	0.000	0.000	0.001	0.001	0.000	0.000	0.000	0.001	0.001	0.000	0.000	0.000	0.000	0.000	0.000
Ca	0.000	0.001	0.001	0.000	0.015	0.002	0.002	0.000	0.000	0.000	0.000	0.000	0.001	0.000	0.000

Text-Fig. 14.
Results of Ar/Ar determination of muscovite mineral ages.

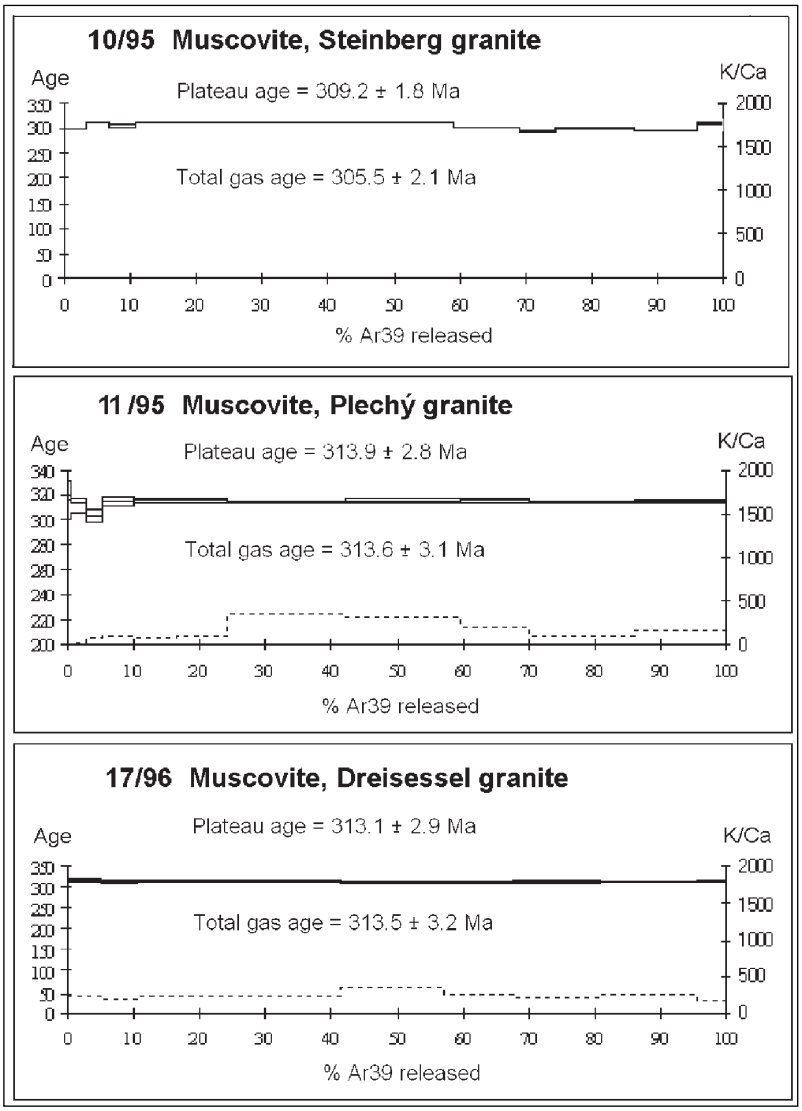

and biotite for considerable long time after solidification or, these parts of the pluton were subjected to a later thermal pulse, i.e. reheating event. Alternatively, at least some of the Rb-Sr mica dates could also be the result of low temperature disturbance of the Rb-Sr system. In case of the low Rb-Sr biotite date of 289 Ma the scatter observed probably reflects Rb-Sr exchange during alteration.

7.2. Relationship between the Granites

All previous investigators distinguished two types of granite in the Plechý pluton, an „equigranular" and a „porphyritic" type. According to our data (rock texture, whole-rock chemistry, mineral chemistry), three granite types can be distinguished:

1) A coarse-grained, equigranular granite,
2) a coarse-grained, serial porphyritic-granite and
3) a hiatal-porphyritic granite with a medium-grained groundmass.

The equigranular and hiatal-porphyritic facies types are easy to distinguish in the field but, in previous studies, the serial-porphyritic facies with variable amount of phenocrysts was classified into one of the beforementioned facies.

The serial-porphyritic „Dreisessel" facies forms the upper part of mountains near the western contact of the pluton – summits of Dreisessel (1311 m), Hochstein (1332 m), Kamenná (979 m) and Ohradec (875 m). A slightly porphyritic variety of the „equigranular" Plechý granite was found on several other hills further to the north. We interpret the Dreisessel facies as near-upper contact rim of the Plechý pluton, slowly passing down into the equigranular Plechý facies.

The Plechý granite, forming the major part of the Plechý pluton, is texturally and chemically homogeneous. It is generally coarse-grained, non-porphyritic, although domains with some larger K-feldspars set in a relatively fine-grained matrix appear slightly porphyritic. Chemically, small differences between the more fractionated northeastern and less fractionated southwestern part of the pluton were found, as can be seen, for example, in the $1/TiO_2$ versus K/Rb diagram (Text-Fig. 15a). The transition between both domains is located along a major fault zone cutting the pluton in NW-SE direction. A small domain containing more fractionated granites was also found near the southeastern contact of the pluton, around the topographically highest point of the pluton, the Plechý/Plöckenstein summit (Text-Fig. 15b). This chemical difference may be due to different denudation rates and/or erosion levels between the northeastern and southwestern portions of the pluton. It is interesting to note that the dykes of fine-grained granite only occur in the less evolved southwestern domain.

The Steinberg granite shows compositional variations in terms of the trace elements Th, Zr, and the REEs; all these elements are positively correlated each other. The highest enrichment of Th, Zr, and REEs (and depletion of Rb) was found along the southern contact of the intrusion, at the village of Schwarzenberg in Austria and southeast of the village of Haidmühle in Germany. This part of the intrusion is also geographically relatively deep-seated (the most eroded?). Towards the north, at a higher geographic elevation, Zr, Th, and REE concentrations slightly decrease whereas the Rb concentration increases.

Similar peraluminous chemical composition and uniform initial $^{87}Sr/^{86}Sr$ isotope ratios of all three granite types suggest close genetic relations. Geological observation implying a younger age of the Steinberg granite compared to the Plechý granite (OTT, 1992) could not be confirmed during our field work. The $^{207}Pb/^{206}Pb$ zircon data (Table 9) are in line with the following order of emplacement: Steinberg –> Dreisessel –> Plechý. From the Steinberg granite to the Dreisessel and Plechý granites, the contents of Si and Na increase, and the contents of Ti, Mg, Fe, K, and compatible trace elements like REE, Zr, and Th decrease. Such evolution is in agreement with the standard model of magma differentiation.

Interestingly, although the Steinberg and Dreisessel granites seem to be slightly older than the Plechý granite, they have higher Rb and F concentrations. This could be explained as follows:

According to experimental work on peraluminous melts, the distribution coefficient of Rb between K-feldspar and melt, $D(Rb)^{Kfs/melt}$, is close to unity (ICENHOWER & LONDON, 1996). For biotite, this distribution coefficient, i.e., $D(Rb)^{Bt/melt}$, is about 2 (ICENHOWER & LONDON, 1995).

Table 9.
Comparison of available geochronological data (reported in million years, Ma) of the Plechý (Plöckenstein) pluton (Ar-Ar by S. SCHARBERT and W. FRANK, Rb-Sr of micas by W. SIEBEL, EMPA by R. ŠKODA and R. ČOPJAKOVÁ).

Sample	Locality	Pb-Pb zircon	Ar-Ar Muscovite	Rb-Sr Muscovite	Ar-Ar Biotite	Rb-Sr Biotite	UThPb Monazite
Plechý granite							
18/96	Jelení		313.5±3.5		313.7±2.7		
19/96	Nová Pec		318.6±3.2		312.7±2.7		
11/95	Oberschwarzenberg		313.9±3.6		311.6±2.6		
12/95	Oberschwarzenberg		315.2±3.2		309.5±2.7		
3623	Jelení			**320 ± 4**		**289 ± 4**	
2283	Trojmezná	**324.6±1.4**					308±14
3854	Rosenbergut						310±19
4370	Stožec			**306 ± 4**			
Dreisessel granite							
17/96	Nové Údolí		313.1±3.1		313.9±2.2		
4365	Kamenná			**322 ± 4**			324±12
4363	Dreisessel	**327.1±1.9**					324±12
Steinberg granite							
10/95	Teufelschüssel		309.2±3.1		308.7±2.4		
4139	Teufelschüssel			**319 ± 4**		**327 ± 4**	307±11
4362	Habergrasberg			**324 ± 4**		**314 ± 4**	
4278	Pendelin						309±13
3698	Habergrasberg	**328.1±1.7**					
3619	Haidmühle						299±12
4367	Špičák			**315 ± 4**			307±16

The Rb-content in muscovite is slightly lower than in biotite. So, early crystallisation and removal of K-feldspar (~30 vol.% of the rock) and biotite (5–10 vol.% of the rock) from the parental melt is not sufficient to explain the decrease of Rb in the later Plechý melt. Instead, it seems more likely, that the uppermost part of the magma reservoir, from which all the granites successively derived, was enriched in Rb prior to intrusion.

Table 10.
Whole-rock Rb-Sr isotopic data.
By S. SCHARBERT, Rb and Sr concentrations determined by isotope dilution analyses and isotopic ratios by mass spectrometry.

Sample	Rb (ppm)	Sr (ppm)	$^{87}Rb/^{86}Sr$	$^{87}Sr/^{86}Sr$	$Sr_{i\ 324\ Ma}$
Plechý granite					
11/95	374	41.6	26.4	0.83592 ±9	0.71418
12/95	354	56.0	18.4	0.79800 ±9	0.71315
18/96	345	57.4	17.6	0.79384 ±9	0.71268
19/96	379	47.3	23.5	0.81903 ±10	0.71066
Dreisessel granite					
17/96	467	30.9	44.6	0.91595 ±12	0.71073
Steinberg granite					
10/95	427	67.1	18.6	0.79826 ±11	0.71249

7.3. Other Th-rich Granites in the Moldanubicum

Thorium is a highly compatible element in peraluminous granitic melts and tends to enter early-crystallising accessory minerals like monazite and zircon. Thus, during crystal fractionation, the thorium content of the melt decreases. The two-mica granites from the Moldanubicum (usually termed as Eisgarn-type s.l.) are geochemically relatively evolved rocks, rich in lithophile (granitophile) elements (Rb, F, U, Sn etc.) and poor in Th (usually 20 ppm, occasionally up to 35 ppm; BREITER & KOLLER [1999]).

The Steinberg granite from the Plechý pluton is an exception. Among other magmatic rocks within the Moldanubicum, only the variety of the Mauthausen granite from Gutau near Freistad is comparable in its Th content (average 60 ppm, max 124 ppm Th; GÖD [1996]) with the Steinberg granite. In both granite types, the major Th-host is monazite and Th-enrichment is

not coupled with enrichment of uranium. Source of thorium and processes, which gave rise to its enrichment in the relative late granite intrusion remain unresolved.

The Th-rich Steinberg granite has been used for construction of many old houses in the village of Oberschwarzenberg. The abundance of Th and its decay products in the Steinberg granite causes large background radiation, and therefore, it is recommended not to longer use this rock as a building material.

8. Conclusions

The Plechý/Plöckenstein pluton consists of three granite types:

1) The Plechý granite sensu stricto – a generally equigranular coarse-grained two-mica granite which forms the major part of the pluton;
2) The Dreisessel granite – a serial porphyritic coarse-grained two-mica granite which represents the remnants of the near-upper contact facies of the Plechý pluton, slowly passing down into the typical equigranular Plechý granite;
3) Steinberg granite – a hiatal porphyritic two-mica granite with medium-grained groundmass and strong alignment of K-feldspar phenocrysts which forms an independent, less differentiated intrusion in the SW and S parts of the pluton.

All granite types are peraluminous (ASI 1.15–1.25). The Plechý and Dreisessel granites are chemically similar to the Eisgarn granite s.s.. The Steinberg granite is remarkably enriched in Zr (130–220 ppm), REE (250–350 ppm total REE) and especially in Th (40–90 ppm). These elements are hosted predominantly in monazite.

All three granites crystallised in a short time interval 328–325 Ma (as indicated by Pb-Pb evaporation ages of zircon). The Steinberg granite appears to be slightly older than the other granite types. Mineral ages obtained by the Ar-Ar and Rb-Sr methods on muscovite and biotite vary over a large time interval (327–309 Ma) indicating that the granites cooled down over a protracted time interval or were locally subjected to later perturbations.

Appendix

Methods of Geochronological Analyses

Rb-Sr analyses (S. SCHARBERT, Wien)

Sr, and Rb concentrations in the whole rock samples were determined by isotope dilution (ID), using HF/HNO_3 (Rb-Sr) mixture for dissolution, and ^{87}Rb-^{84}Sr spike, respectively (SCHARBERT & VESELÁ, 1990). Total procedural blanks were <1 ng for Rb and Sr. Rb and Sr concentration (ID) samples were loaded on a single Ta filament and measured on a MICROMASS® M30 machine. Sr isotopic compositions (IC) were run on a Re single filament, using a FINNIGAN® MAT262 mass spectrometer. $^{87}Sr/^{86}Sr$ ratios for NBS987 (Sr) international standard during the course of this work were 0.71014±3. Errors for the $^{87}Rb/^{86}Sr$ ratios are taken as ±1%, or smaller, based on iterative sample analysis and spike recalibration. Isochron calculation was done according to Ludwig (1999). Ages are based on decay constants of 1.42×10^{-11} a^{-1} for ^{87}Rb.

Ar-Ar analyses (W. FRANK, S. SCHARBERT, Wien)

For Ar-Ar age determinations the mineral concentrates were irradiated at the 9MW ASTRA reactor at the Austrian Research Centre Seibersdorf and analysed using standard procedures with a VG-5400 Fisons Isotopes mass spectrometer. Age calculation was done after corrections for mass discrimination and radioactive decay using the formulas given in DALRYMPLE et al. (1984). J-values are determined with internal laboratory standards, calibrated by international standards including muscovite Bern 4M (BURGHELE, 1987) and amphibole MMhb-1 (SAMPSON & ALEXANDER, 1987). The errors given on the calculated age of an individual step include only 1σ error of analytical data. The error of the plateau and total gas ages includes an additional error of ±0.4% on the J-value, based on standard reproducibility (more in SCHUSTER et al., 2001).

Rb-Sr analyses (W. SIEBEL, Tübingen)

For Rb-Sr isotope analyses samples were spiked with a mixed ^{84}Sr-^{87}Rb tracer solution and dissolved in 52% HF for four days at 130°C on a hot plate (whole-rock samples) and in pressure vessels (muscovite, biotite). Digested samples were dried and re-dissolved in 6N HCL, dried again and re-dissolved in 2.5N HCl. Rb and Sr were isolated on quartz columns by conventional ion exchange chromatography with a 5 ml resin bed of Bio Rad AG 50W-X12, 200-400 mesh. All isotopic measurements were made by Thermal Ionization Mass Spectrometry, on a Finnigan MAT 262 mass spectrometer at Tübingen University. Sr was loaded with a Ta-HF activator on pre-conditioned W filaments and was measured in single-filament mode. Rb was loaded with ultra-pure H_2O on pre-conditioned Re filaments and measurements were performed in a Re double filament configuration. The $^{87}Sr/^{86}Sr$ isotope ratios were normalised to $^{86}Sr/^{88}Sr = 0.1194$. Analyses of 15 separate loads of the NBS 987 Sr standard, during the course of this study (01-07/2006) gave a $^{87}Sr/^{86}Sr$ ratio of 0.710254 ± 0.000014 (reference value = 0.710248). Blank (chemistry and loading) was 200 pg for Sr.

UThPb microprobe analyses (R. ŠKODA, Brno)

Monazite was examined using a CAMECA SX 100 electron microprobe. Operating conditions were: an accelerating voltage 15

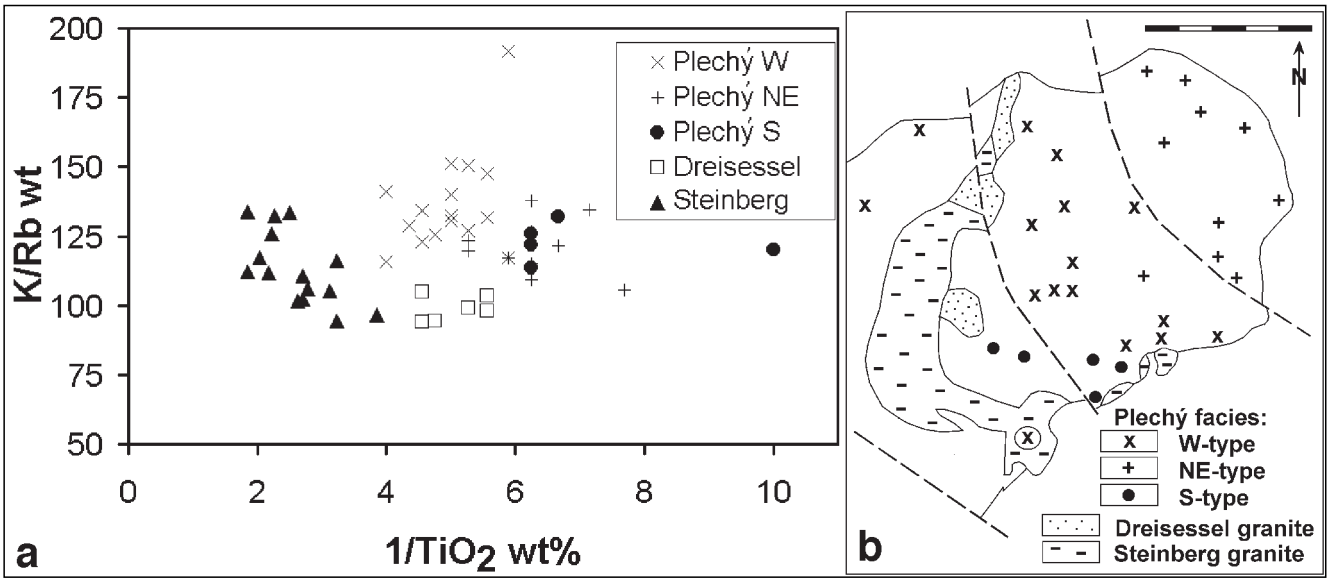

Text-Fig. 15.
Internal differences within the Plechý granite (a: K/Rb versus $1/TiO_2$ diagram; b: subdomains of the Plechý granite).

kV, a beam current of 80 nA and a beam diameter of <1 μm. Peak counting times were 20 s for major elements and 30–60 s for majority of minor elements. Uranium was determined on the U M_β line (counting time 60 s, detection limit 270 ppm), thorium on the Th M_α line (counting time 40 s, detection limit 250 ppm) and lead on the Pb M_α line (counting time 240 s, detection limit 130 ppm). Data were reduced using the PAP matrix correction routine (POUCHOU & PICHOIR, 1985). Concentrations of Pb were additionally manually corrected for Y $L_{\gamma 2}$, Th $M_{\zeta 1}$ and $Th_{\zeta 2}$ overlap on Pb M_α. Besides mentioned coincidentions, the analytical precision of Pb on the M_α line is higher than on M_β line where only insignificant coincidention occurs. Microprobe monazite analyses were used for monazite dating (CHIME – chemical Th-U-total Pb isochron method) provided that all Pb is radiogennic (PARRISH, 1990). The monazite age was calculated with the method of MONTEL et al. (1996).

Acknowledgement

This work was supported by the Austrian-Czech cooperation program AKTION-KONTAKT, projects 2001-2 and 2005-2. Field measurement of the radioactivity was supported also in the frame of bilateral cooperation between the Geologische Bundesanstalt Wien and Czech Geological Survey Praha, partly also by the geological mapping program of the Czech Geological Survey (project No. 6335 in 2003). Final compilation of this manuscript was supported by the institute research project No. AV0Z30130516 "Earth system at the intersection of geological processes ... " at the Geological Institute of Academy of Sciences of the Czech Republic.

Support of R. ČOPJAKOVÁ (Brno), V. BÖHMOVÁ and Z. KORBELOVÁ (Praha) and T. NTAFLOS (Wien) during microprobe analyses, F. VESELOVSKÝ (Praha) during mica separation and E. REITTER (Tübingen) during Sr isotope analyses is cordially acknowledged.

Careful review of an earlier version of the manuscript by H.-J. Förster (Potsdam) help us to improve the article and is with thanks acknowledged.

Literature

BLÍŽKOVSKÝ, M. & NOVOTNÝ, A. (1982): Gravity map of the Bohemian Massif. – MS Geofyzika n.p. Brno.

BREITER, K. & KOLLER, F. (1999): Two-mica granites in the central part of the South Bohemian pluton. – Geologie ohne Grenzen. Festschrift 150 Jahre Geologische Bundesanstalt, Abh. Geol. B.-A., **56**, 201–212.

BREITER, K. & KOLLER, F. (2005): New interesting types of granitoids in the three-corner-country (Dreiländereck) of Austria, Czech Republic and Germany. – Mitt. Österr. Miner. Ges., **151**, 33.

BREITER, K. (2005): Short note on a Thorium-rich granite in the Three Corner Area (Dreiländereck) of Austria, Czech Republic and Germany. – Jb. Geol. B.-A., **145**, 141–143.

BREITER, K. & PERTOLDOVÁ, J. (2004): Interesting granitoids in the border area of the Czech Republic, Austria and Bavaria. – Ber. Inst. Erdwiss. K.-F.-Univ. Graz, **9**, 91–93.

BURGHELE, A. (1987): Propagation of error and choice of standard in the $^{40}Ar/^{39}Ar$ technique. – Chem. Geol., **66**, 17–19.

DALRYMPLE, G.B., ALEXANDER, E.C., LANPHER, M.A. & KRAKER, G.P. (1984): Irradiation of samples for $^{40}Ar/^{39}Ar$ dating using the Geological Survey TRIGA reactor. – U.S. Geological Survey Professional Papers, **1176**, 1–55, Reston (U.S. Geological Survey).

FÖRSTER, H-J., TISCHENDORF, G., TRUMBULL, R.B. & GOTTESMANN, B. (1999): Late-collisional granites in the Variscan Erzgebirge, Germany. – Journal of Petrology, **40**, 1613–1645.

GÖD, R., OBERLERCHER, G. & BRANDSTÄTTER, F. (1996): Zur Geochemie und Mineralogie eines Monazit-führenden Granitkörpers im Südböhmischen Pluton (Gutau, Oberösterreich). – Jb. Geol. B.-A., **139**, 445–452.

Icenhower, J., London, D. (1995): An experimental study of element partitioning among biotite, muscovite, and coexisting peraluminous silicic melt at 200 Mpa (H_2O). Amer. Mineralogist, 80, 1229–1251.

ICENHOWER, J. & LONDON, D. (1996): Experimental partitioning of Rb, Cs, Sr, and Ba between alkali feldspar and peraluminous melt. – Amer. Mineralogist, **81**, 719–734.

LUDWIG, K.R. (1999): User`s manual for Isoplot/Ex version 2.2, A. Geochronological toolkit for Microsoft Excel. – Berkeley Geochronology Center Special Publ., **1a**, 53 pp.

MIKSA, V. & OPLETAL, M. (1995): Geological map of the Czech Republic on a scale 1 : 50 000, sheet 32-14 Nová Pec. – Praha (Czech Geological Survey).

MONTEL, J.M., FORET, S., VESCHAMBRE, M., NICOLLET, C. & PROVOST, A., (1996): Electron microprobe dating of monazite. – Chemical Geol., **131**, 37–53.

OTT, W.D. (1992): Geologische Karte von Bayern 1 : 25 000, Erläuterungen zum Blatt Nr. 7248/49 Jandelsbrunn. – 72 pp., München.

PARRISH, R.R. (1990): U-Pb dating of monazite and its application to geological problems. – Canad. J. Earth Sci., **27**, 1431–1450.

PERTOLDOVÁ, J. et al. (2006): Geological map of the Czech Republic in scale of 1 : 25 000, sheet 32-141 Nové Údolí and 32-142 Nová Pec. – MS Czech Geological Survey Praha.

PERTOLDOVÁ, J., BREITER, K. & SULOVSKÝ, P. (2004): Granites in the border area of the Czech Republic, Austria and Bavaria. – Geoscience Research Reports for 2003, 30–33, Praha (Český geologický ústav). In Czech with English abstract.

POUCHOU, J.L. & PICHOIR, F. (1985): „PAP" procedure for improved quantitative microanalysis. – Microbeam Analysis, **20**, 104–105.

SAMPSON, S.D. & ALEXANDER, E.C. (1987): Calibration of the interlaboratory $^{40}Ar/^{39}Ar$ dating standard, Mmhb-1. – Chemical Geology, **66**, 27–34.

SCHARBERT, S. & VESELÁ, M. (1990): Rb-Sr systematics of intrusive rocks from the Moldanubicum around Jihlava. – In: MINAŘÍKOVÁ, D. & LOBITZER, H. (eds): Thirty years of cooperation between Austria and Czechoslovakia, Festive Volume, Vienna (GBA) – Praha (ČGÚ).

SCHUSTER, R., SCHARBERT, S., ABART, R. & FRANK, W. (2001): Permo-Triassic extension and related HAT/LP metamorphism in the Austroalpine – Southalpine realm. – Mitt. Ges. Geol. Bergbaustud. Österr., **45**, 111–141, Wien.

SIEBEL, W. (1993): Der Leuchtenberger Granit und seine assoziierten magmatischen Gesteine: Zeitliche und stoffliche Entwicklungsprozesse im Verlauf der Entstehung des Nordoberpfalz-Pluton. – Inaugural-Dissertation Ruprecht-Karls-Universität Heidelberg, 308 pp.

THIELE, O. & FUCHS, G. (1965): Übersichtskarte des Kristallins im westlichen Mühlviertel und im Sauwald, Oberösterreich. – Wien (Geol. B.-A.).

Manuskript bei der Schriftleitung eingelangt am 15. Oktober 2007